NASA Technical Memorandum 4223

Concept Development of a Mach 4 High-Speed Civil Transport

Christopher S. Domack, Samuel M. Dollyhigh,
Fred L. Beissner, Jr., Karl A. Geiselhart,
Marvin E. McGraw, Jr., Elwood W. Shields,
and Edward E. Swanson

DECEMBER 1990

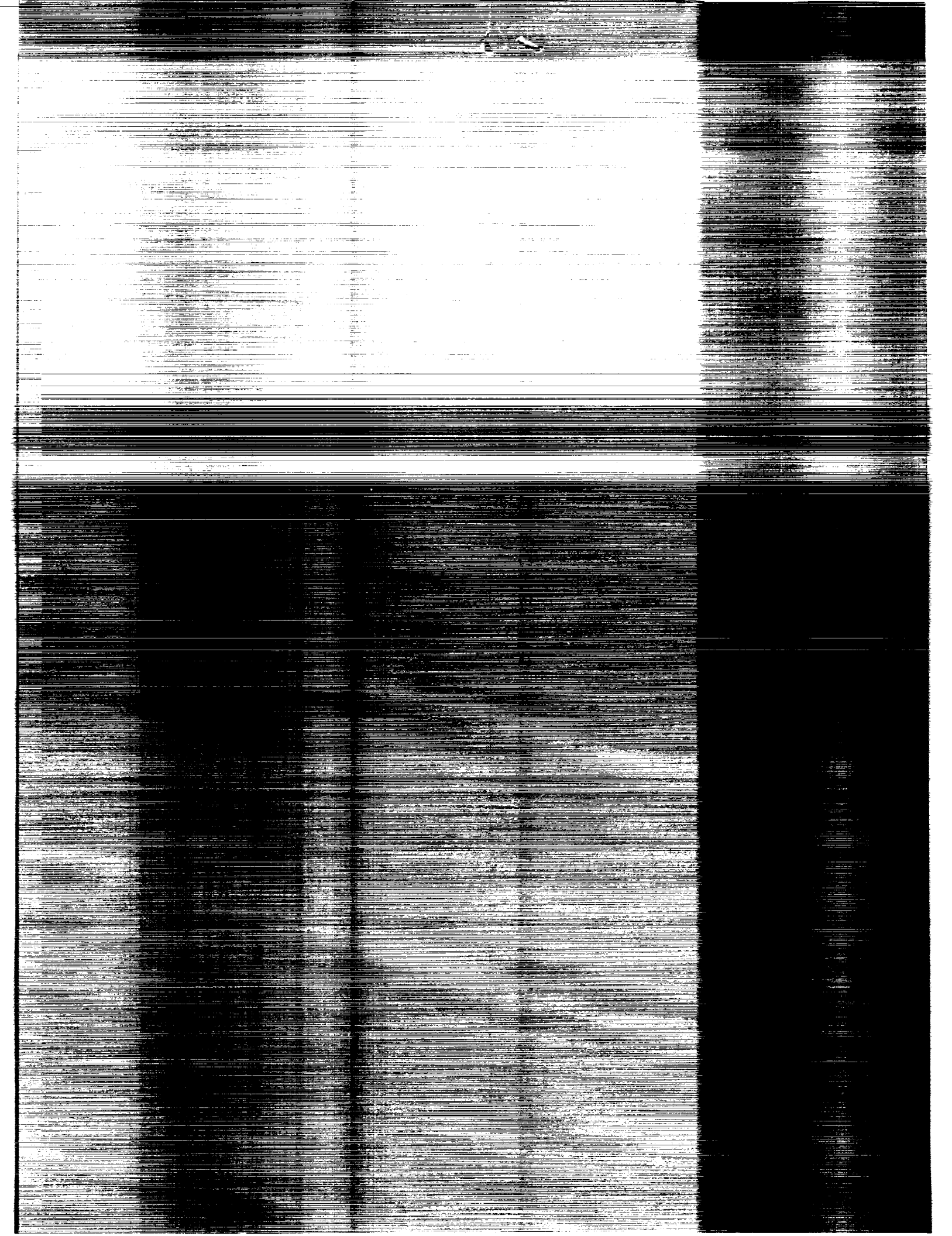

NASA Technical Memorandum 4223

Concept Development of a Mach 4 High-Speed Civil Transport

Christopher S. Domack
Lockheed Engineering & Sciences Company
Hampton, Virginia

Samuel M. Dollyhigh
Langley Research Center
Hampton, Virginia

Fred L. Beissner, Jr., Karl A. Geiselhart,
Marvin E. McGraw, Jr., and Elwood W. Shields
Lockheed Engineering & Sciences Company
Hampton, Virginia

Edward E. Swanson
Planning Research Corporation
Hampton, Virginia

National Aeronautics and
Space Administration
Office of Management
Scientific and Technical
Information Division

1990

Summary

A study was conducted to configure and analyze a 250-passenger, Mach 4 high-speed civil transport with a design range of 6500 n. mi. The design mission assumed an all-supersonic cruise segment and no community noise or sonic boom constraints. The study airplane was developed in order to examine the technology requirements for such a vehicle and to provide an unconstrained baseline from which to assess changes in technology levels, sonic boom limits, or community noise constraints in future studies. The propulsion, structures, and materials technologies used in the sizing of the study airplane were assumed to represent a technology availability date of 2015. The study airplane was a derivative of a previously developed Mach 3 concept and used advanced afterburning turbojet engines and passive airframe thermal protection. Details of the configuration development, aerodynamic design, propulsion system, mass properties, and mission performance are presented. The study airplane was estimated to weigh approximately 866 000 lb. Although an airplane of this size is a marginally acceptable candidate to fit into the world airport infrastructure, it was concluded that the inclusion of community noise or sonic boom constraints would quickly cause the aircraft to grow beyond acceptable limits with the technology levels assumed in the study.

Introduction

A report by the Office of Science and Technology Policy (OSTP), Executive Office of the President (ref. 1), has identified the technology development to support a long-range supersonic transport as one of three high-payoff national goals advocated to sustain the nation's leadership position in aeronautics. It recommended that the American aerospace industry and NASA determine the most attractive technical concepts and the necessary technology developments to enable such an aircraft. As described in reference 2, NASA has conducted research on a continuing basis that is applicable to sustained supersonic cruise aircraft and, in response to the OSTP recommendations, is conducting technology integration studies focused on the feasibility of a long-range, high-speed civil transport (HSCT).

The first phase of the current HSCT study program involved an examination of the factors influencing the choice of design Mach number and range, including assessment of the feasibility of vehicle concepts for different levels of technology. The results of one of these HSCT technology integration studies were reported in reference 3, a Mach 3 configuration study that subsequently formed the basis for the current Mach 4 effort. The current study sought to examine how the additional technical difficulties involved in flying at Mach 4 influenced the viability of the vehicle considering the reduction in travel time possible compared with a slower vehicle.

Analysis of the worldwide airline route structure reported in reference 4 indicates that an aircraft with a range slightly in excess of 6000 n. mi. could fly 90 percent of the long-range market routes. After an examination of major international city pairs, a design range of 6500 n. mi. was chosen for the HSCT studies. As indicated in figure 1, taken from reference 2, there is relatively little reduction in block time (the time required to travel from the departure gate to the arrival gate) to fly a mission of 6500 n. mi. at cruise Mach numbers above 5. This is because the time spent in ground operations and in acceleration and deceleration becomes a greater fraction of the total mission time as the cruise Mach number increases. Implicit in this figure is that the reduction in block time for flying the transpacific mission at Mach 4 as opposed to Mach 3 is quite small, on the order of only 30 minutes. Current subsonic transports flying long-range routes such as those to the Pacific Basin require block times of 12 to 14 hours. In comparison, a vehicle with Mach 4 cruise capability would require less than 4 hours to fly the same mission. Projected trends (ref. 4) predict that travel on these routes will increase at a rate three times that forecast for the North Atlantic routes. As travel and trade with the Pacific Basin nations increase, so will the demand for more productive, less time-consuming air transportation. Nevertheless, the potential time savings need to be carefully weighed against the technical difficulties involved in order to produce a viable commercial vehicle.

The Mach 4 HSCT concept reported herein represents a level of technology assumed to be available for production by the year 2015. The concept serves as a benchmark in the ongoing series of NASA HSCT technology integration and feasibility studies from which assessments of the impact of changes in technology levels or requirements such as community noise or sonic boom limits may be made. According to references 4, 5, and 6, Mach 4 represents an approximate upper limit to the applicability of JP-fueled turbojet engines and simple thermal management systems. The concept thus employs advanced afterburning turbojet engines and passive thermal management; that is, thermal protection and control are accomplished by means of insulation rather than actively circulating coolant through the airframe. It is recognized that several design features of the concept would require challenging and aggressive technology development programs in order to meet the

projected technology availability date. Details of the configuration development, aerodynamic design, propulsion system, mass properties, and mission performance are presented.

Symbols

C_D	drag coefficient, D/qS
C_{D_L}	drag due to lift
C_{D_0}	zero-lift drag coefficient
C_L	lift coefficient, L/qS
c	airfoil local chord length, ft
$\bar{c}$	mean aerodynamic chord length, ft
D	drag, lb
h	altitude, ft
L	lift, lb
M	Mach number
q	dynamic pressure, lb/ft^2
R/R_G	mission range as fraction of Earth's circumference
S_{ref}	reference wing area, ft^2
$\overline{S}(x)$	average equivalent body cross-sectional area, ft^2
t	airfoil thickness, ft
x	longitudinal distance along fuselage from nose, ft

Abbreviations:

c.g.	center of gravity
DGW	design gross weight, lb
EW	empty weight, lb
FAR	Federal Aviation Regulations
FS	fuselage station, in.
LE	leading edge
OW	operating weight, lb
SFC	specific fuel consumption, $\frac{lb/hr}{lb}$
ZFW	zero fuel weight, lb

Configuration Description

The study airplane is a Mach 4 derivative of the Mach 3 concept originally presented in reference 3. The general arrangement of the airplane is illustrated in figure 2; principal geometric dimensions are presented in table I. The concept employs a blended wing-body with a modified platypus nose, a highly swept inboard wing panel, and a moderately swept outboard wing panel with curved, raked wingtips. This wing planform was selected to minimize induced drag (inversely proportional to span squared) and wave drag due to lift (inversely proportional to lifting length squared) while maintaining adequate low-speed aerodynamic characteristics. The compound leading-edge planform provides a minimal shift in aerodynamic center location between takeoff and supersonic cruise speeds, and the lifting forewing can provide favorable flap-trimming pitching moments.

The inboard wing panel is swept 80°, allowing the flow component normal to its leading edge to remain subsonic even at the Mach 4 cruise condition. The high sweep allows relatively blunt leading edges without a substantial zero-lift wave drag penalty. These features result in an insensitivity of optimum leading-edge camber to flight speed and of airfoil section performance to camber. This allows the inboard leading edge to have fixed geometry, free of high-lift devices, resulting in a simpler and lighter wing structure.

The outboard wing panel is swept 53° and incorporates a curved, raked wingtip planform. At low speeds and high angles of attack, flow separation at the wingtip is common and tends to produce a severe pitch-up. Reference 7 indicates that a curved wingtip planform tends to relieve this problem through controlled vortex separation. Other investigators (refs. 8 to 10) have found that wings with curved tips also exhibit improved induced drag characteristics. Another device incorporated to improve the low-speed aerodynamics of the planform is the leading-edge notch flap. This is a device intended to help retain potential flow on the outboard wing panel while the inboard panel flow is unavoidably three-dimensional. The deflected notch flap serves as a pylon vortex generator, the operation of which is detailed in reference 11. Preliminary water-tunnel tests of this planform indicate that the notch flap operates as postulated.

Other high-lift devices used in the design include 15 percent chord leading-edge flaps on the outboard panel, 25 percent chord trailing-edge flaps, and deflected engine nozzles. The nozzles on the configuration are set at 5° downward deflection and located close to the wing trailing edge so that the gross thrust vector develops not only a lift component but also some supercirculation at subsonic speeds.

The airfoil thickness-chord ratios (t/c) and the spanwise thickness distribution of the wing of the Mach 4 configuration differ from those of the Mach 3 concept. The principal differences consist of slightly

increased t/c for the inboard wing sections and reduced t/c for the outboard panels. The increased thickness inboard provides additional volume for fuel tanks and insulation. Because of the more severe aerodynamic heating environment, the thinner outboard panel was assumed to carry no fuel.

The forebody of the concept is slender and elliptical in cross section. Reference 12 indicates that the directional stability of elliptical forebodies is superior to that of more conventional circular shapes at high angles of attack. As may be seen from the interior arrangement drawing presented in figure 3 , the length of the forebody and the span of the forewing at the crew station would prohibit meeting conventional external vision requirements without a variable geometry (droop-snoot) forebody. A see-by-wire system was chosen in lieu of a droop-snoot forebody and windows for several reasons. Using multiple displays similar to current flight simulator practice, such a system could provide information in both the visible and invisible spectra (e.g., radar and infrared), enhancing visibility and safety at night and in adverse weather. Ground operations would also benefit from the availability of multiple camera locations.

The main cabin is configured for 250 passengers in 3 to 6 abreast seating at 34 in. pitch. Six lavatories are provided, with two forward and four in the aft cabin. The main entrance doors are located on each side of the fuselage between the aft lavatories and the galley, and three emergency exits are provided over each wing. Like the cockpit, the main cabin is windowless. The lack of windows simplifies the fuselage structural design and environmental control. Outside visibility and entertainment for the passengers would be provided by individual seat-back video systems similar to those now entering commercial service.

The main landing gear is a two-strut arrangement with six wheels per strut. The wing-mounted struts retract into the engine nacelles and are housed between the inlet ducts. The two-wheeled nose gear is mounted on the bulkhead forward of the crew station and retracts forward. Each landing gear strut is a dual-acting hydraulic cylinder, with one action to absorb landing shocks and a second to provide strut compression for stowage.

Four advanced afterburning turbojet engines are mounted in two nacelles on the wing lower surface adjacent to the fuselage. This allows the engine mounting structure to utilize the fuselage structure to increase stiffness and improve wing flutter boundaries. The location of the engine nacelles provides for favorable lift and drag interference between the nacelles and the lower surface of the configuration. A boundary-layer diverter on each nacelle directs the boundary-layer flow to the outside of the engines in the conventional manner. Engine-driven accessories are located in the fuselage below the cabin between the wing spar carry-through and the aft fuselage fuel tank and are driven through a remote gearbox by extension shafting from the engines. The subsystems powered include environmental control, hydraulics, and the electrical system. An auxiliary power unit for self-contained ground operation is also located in this area. Fuel is carried in 24 integral wing tanks and 1 aft fuselage tank. The aft fuselage tank is used primarily for aircraft center-of-gravity management.

Aerothermal Analysis

Aerothermal considerations affect the design and operation of any supersonic-cruise vehicle. As design Mach number increases, management of aerodynamic heating forces the propulsion system cycle selection and airframe aerodynamic and structural designs to become more critically linked. The principal reasons for this increased interdependence are the utilization of the aircraft fuel supply as a heat sink and the integration of vehicle surfaces with the inlet and nozzle systems.

As discussed in more detail in references 3 through 5, one of the most important considerations in the current series of HSCT studies is the selection of fuel for the vehicle. Fuels considered in prior studies have included conventional jet fuel (e.g., Jet A, JP-4), thermally stabilized jet fuel (TSJF), methane, endothermic fuels (methycyclohexane, Decalin), and cryogenic fuels such as hydrogen. While methane, endothermic, and cryogenic fuels have some attractive features from propulsion and aerothermal management standpoints, they introduce a host of other complications in the practical aspects of economics and compatibility with the existing world airport infrastructure. Given these complications and the fact that the existing airport infrastructure is designed around conventional jet fuel, it was assumed for the current study that the vehicle would use TSJF.

A passive thermal management system was assumed for the study airplane; that is, the structure and contents of the airplane are protected from the aerothermal environment by insulation. Another design option was to use an active airframe cooling system, one in which a fluid medium (usually the fuel) is circulated throughout the airframe and then burned by the engines or returned to storage. The active cooling approach appears to promise structures that are lighter and more volumetrically efficient than passively insulated ones, but the passive approach was chosen for this study for two primary reasons: safety and economy. It was reasoned that the relative simplicity of a passive system would lead to advantages

in both safety and cost, each vital to the success of a commercial vehicle.

The insulation thickness required for a passive system is principally a function of heating rate, insulating material properties, and time of exposure to heating. A first-order thermal analysis of the study configuration was performed in which local heating rates and skin temperatures were estimated for various locations on the aircraft. The insulation requirements were then determined after establishing limiting local interior wall temperatures at the end of the design mission.

The exterior skin temperature analysis was performed using a time-dependent energy balance approach. Empirical relationships (modified Reynolds analogies) presented in references 13 and 14 were employed to predict frictional heating rates. This procedure allowed the vehicle to be approximated as a combination of simple geometric shapes such as flat plates, cylinders, and cones. Figure 4 presents a sampling of exterior skin temperatures calculated at various locations on the study vehicle for a midcruise flight condition. The insulation thickness solution was obtained by treating the local conditions individually as a one-dimensional transient conduction problem and solving the resulting partial differential equation numerically using the method presented in reference 15. Limiting interior wall temperatures of 100°F for the cabin and 250°F for the wing fuel tanks were used in the analysis, and an advanced, lightweight insulating material with thermal properties similar to that of quartz fiber was assumed. The resulting combined structure and insulation thickness used in calculation of the airframe weight and available fuel volume was 9 in. for the cabin walls and 3 in. for the wing fuel tanks.

Mass Properties

Estimation of the study airplane weight and balance was performed using an empirically based transport aircraft weight analysis routine incorporated in the aircraft performance and sizing computer program of reference 16. The weight estimation formulas used within the program were developed from a data base of current transport aircraft having conventional aluminum and titanium construction and conventional subsystems technology. A multiplication factor was then applied to each formula to account for improvements in technology that would effect a weight reduction.

For this study, several areas of technology improvement were assumed to represent the year 2015 technology availability date. The fuselage and primary wing structure are constructed of superplastically formed, diffusion-bonded (SPF/DB) titanium. Wing secondary structure, including fairings, control surfaces, and fuel tanks, is made of advanced composite material such as graphite/polyimide. For the landing gear, radial-ply tires, lightweight forged wheels, and carbon brakes are used. The hydraulic system weight is based on a 5000-psi operating pressure with titanium lines and fittings. For the remaining subsystems, such as electrical, instruments and avionics, auxiliary power, and environmental control, a technology improvement factor of 15 to 20 percent over current systems was assumed.

A summary weight statement for the study configuration is presented in table II, and the corresponding center-of-gravity diagram is illustrated in figure 5.

Aerodynamics

Zero-Lift Drag

The zero-lift drag characteristics for the study configuration are shown as a function of Mach number in figure 6. Values are presented corresponding to altitudes of 40 000 and 80 000 ft in order to represent typical subsonic and supersonic operating conditions. The drag buildup analysis began with fully turbulent boundary-layer skin-friction drag values calculated using the T' method of Sommer and Short (ref. 17). Subsequently, form drag was calculated by application of geometry-dependent form factors as defined in reference 18. Roughness drag was estimated using an unpublished empirical method and amounted to approximately 4.5 percent of the combined friction and form drag. The zero-lift wave drag (wave drag due to volume) of the study configuration was computed using the far-field method of reference 19; this method includes the ability to define a minimum wave drag fuselage area distribution through a set of constraining fuselage stations at a given Mach number. It was recognized that Mach 4 is at the upper limit for which linearized supersonic aerodynamic analysis methods should be considered; however, because of the slenderness of the configuration the levels and trends with Mach number should be valid. The numerical model used in the wave drag evaluation is presented in the format of reference 20 in table III. The Mach 4 average equivalent body area buildup for the airplane concept is presented in figure 7.

Lift-Dependent Drag

Subsonic lift-dependent drag was calculated using the method of reference 21, which accounts for the effects of attainable leading-edge thrust and vortex lift. A lift-dependent drag improvement due to the 5° turning of the internal flow within the engine nacelles prior to exhaust nozzle entry was taken in place

of any propulsion-induced supercirculation lift from the deflected nozzle flow. Mission-adaptive wing flap deflection schedules similar to those described in reference 3 for the Mach 3 configuration were prepared; the flap deflection schedules were then used to prepare envelope drag polars for the current study configuration. A detailed discussion of the development of these flap deflection schedules is contained in reference 22. Representative drag polars for several subsonic Mach numbers are presented in figure 8.

Supersonic lift-dependent drag was evaluated by the modified linear-theory method of references 23 through 25. The wing camber and twist definition were also designed using methods contained in this series of documents. The numerical model used in the analyses is presented in the format of reference 20 in table IV. The portion of the fuselage aft of the wing trailing edge at the configuration centerline is not included in this model definition since the analysis code is concerned only with lifting surfaces. The lift-dependent drag at several supersonic Mach numbers is shown as a function of lift coefficient in figure 9. The net lift-dependent drag values presented take into consideration attainable leading-edge thrust (see ref. 22) and improvements due to optimization of the wing camber and twist. Typical trimmed supersonic total-drag polars are shown in figure 10 for Mach numbers of 1.4, 2.2, 3.2, and 4.0.

Maximum Lift-Drag Ratio

The variation of maximum trimmed lift-drag ratio versus Mach number is presented in figure 11 for altitudes of 40 000 and 80 000 ft in order to represent typical subsonic and supersonic cruise conditions. Maximum values vary from approximately 13.7 at high subsonic cruise to 7.3 at the Mach 4 design condition.

Trim Considerations

The variation of aerodynamic center location with Mach number is illustrated in figure 12. The rapid forward movement with increasing supersonic speed is probably associated with an increasing lift-curve slope of the inboard portion of the wing as its leading edge becomes nearly sonic, while the lift-curve slope of the supersonic-leading-edge outboard panel remains nearly constant. The pitch trimming capability of the concept is aided by the large positive zero-lift pitching moments provided by the "lifting platypus" forebody of the planform.

The extent to which center of gravity may be moved aft for pitch trim in supersonic cruise is often dependent on the level of directional stability available. The vertical tail area of the current study configuration was increased over that of the Mach 3 baseline configuration in recognition of the substantially larger engines and nacelles of the current concept. Given the high levels of stability augmentation possible with advanced flight control technology, the configuration should demonstrate adequate directional stability throughout its speed range.

Propulsion

The propulsion system selected for this study consists of four conceptual single-rotor, augmented (afterburning) turbojets using thermally stabilized jet fuel. A technology readiness date of 2015 was assumed for the engine, and no noise constraints were imposed on its design. The engine uses a two-dimensional, variable-geometry, mixed-compression inlet and a two-dimensional, variable-geometry, convergent-divergent nozzle with thrust reversing. It was designed for optimum performance at the cruise point of Mach 4 at an altitude of approximately 75 000 ft. The uninstalled performance characteristics for the engine were computed using techniques based on those described in reference 26. Installed engine performance data, including the effects of inlet pressure recovery, inlet spillage drag, and nozzle boattail drag, were computed using the techniques described in reference 27. The geometry of the engine for scaling purposes is presented in figure 13.

The engine has an installed thrust-weight ratio of 8.1 at maximum afterburning operation. Each develops a sea level static thrust of 111 000 lb at maximum afterburning operation and 59 682 lb at maximum dry (nonafterburning) operation. The sea level static airflow for the engine is 795 lb/sec, and the overall pressure ratio is 15.0. The turbine inlet temperature is limited to 3500°R, and a combustor efficiency of 99 percent is assumed. The compressor and turbine peak adiabatic efficiencies are 87 and 91 percent, respectively; at cruise these efficiencies are slightly lower. In order to simulate the effect of the vehicle forebody on the propulsion system, the inlet sizing and engine performance data include the effective precompression resulting from a 7° wedge in the free stream. The free-stream pressure recovery of the inlet used in this analysis is based on pressure recovery as a function of Mach number of the Mach 3.5 two-dimensional, mixed-compression inlet presented in reference 28. The study engine inlet has a cruise point total pressure recovery, including precompression, of 0.85. A nozzle velocity coefficient of 0.99 was used throughout. A breakdown of the propulsion system losses is presented in figure 14. The cruise point installed specific fuel consumption for the

engine ranges from 1.63 $\frac{\text{lb/hr}}{\text{lb}}$ for maximum dry operation to 2.29 $\frac{\text{lb/hr}}{\text{lb}}$ at maximum afterburning. This yields a maximum dry cruise point overall efficiency of 59.6 percent. The installed performance characteristics of the engine are summarized in figures 15 and 16.

Mission Performance

This section presents an estimate of the performance capabilities of the concept and the results of computing the wing area and engine size required for minimum takeoff gross weight to perform the design mission. No environmental constraints such as takeoff and landing noise abatement procedures or sonic boom overpressure limits were included in the performance and sizing analyses. The intent of the current study was to provide an unconstrained baseline against which the effect of the inclusion of these constraints could be examined in further studies should the concept warrant continued development.

Mission performance and sizing computations were conducted using the Flight Optimization System computer program described in reference 16. The design mission included

A. Fuel for 10 min at idle power for warm-up and taxi out.
B. Fuel to perform the calculated takeoff maneuver to the start of climb condition at maximum afterburning power.
C. Time, distance, and fuel (TDF) for minimum-fuel climb to the start of cruise condition. Power setting variable from maximum dry to maximum afterburning.
D. TDF for cruise at Mach 4, best altitude.
E. TDF for calculated descent at maximum L/D, zero thrust, idle fuel flow.
F. Reserve fuel allowance (no range credit) consisting of
    1. Fuel required for missed approach estimated as fuel to accelerate from power-off stall speed to beginning of reserve climb path (Mach 0.3, $h = 0$) at maximum afterburning thrust at calculated end-of-trip weight.
    2. Fuel required for minimum-fuel climb to reserve cruise condition.
    3. TDF for cruise at best subsonic Mach number and altitude. Required range 250 n. mi. including distance for climb and descent.
    4. Fuel for 30 min hold at Mach number and altitude for minimum fuel flow.
    5. TDF for calculated descent at maximum L/D, zero thrust, idle fuel flow.
    6. Additional fuel reserve allowance of 5 percent of total trip fuel (C, D, and E above).
G. No TDF credit or penalty for approach, landing, or taxi in.

Takeoff distance and one-engine-inoperative climb margins during takeoff and missed approach were based on maximum dry (nonafterburning) power. However, for conservatism, the mission performance fuel burns include estimates of the fuel required for takeoff and missed approach using full afterburning power. The climb and descent profiles used in the mission are illustrated in figure 17. The effect of the Earth's rotation was not accounted for, and all calculations were carried out at standard, no-wind atmospheric conditions.

Figure 18 presents a thumbprint sizing plot, which consists of contours of constant takeoff gross weight imposed on a grid of aircraft wing area versus engine size. All the potential configurations represented on the thumbprint contours meet the design mission range of 6500 n. mi. Also shown on the figure are lines indicating specific values for design constraints, including landing field length, internal fuel volume limit, and landing approach speed. The constraint lines delimit designs that are feasible under the specified performance requirements and were used to determine the minimum takeoff gross weight configuration to perform the design mission. The selection criteria applied to the study configuration included a 10 000-ft takeoff and landing field length limit, FAR 25 requirements for one-engine-inoperative second-segment climb and missed approach climb capability, a landing approach speed limit of 160 knots at design landing weight (75 percent of design gross weight), and sufficient internal fuel volume for the design mission including reserves. Applicable criteria are indicated on the thumbprint sizing plot.

The thumbprint plot indicated a minimum gross weight of approximately 865 700 lb would be necessary to perform the design mission. This "sized" aircraft has a wing area of 12 700 ft^2, with engines rated at 111 000 lb sea level static thrust each. This results in a wing loading of 68 lb/ft^2 at design gross weight, a thrust-weight ratio of 0.51 at maximum afterburning power, and a dry thrust-weight ratio of 0.28. The normal end-of-mission approach speed and landing distance for the sized configuration are 128 knots and 6994 ft, respectively, at a landing weight of 420 742 lb. This weight includes a reserve fuel allowance of 57 513 lb. The corresponding primary mission summary is presented in table V, with the reserve mission summarized in table VI. Note that minor reconfiguration of the study airplane would be necessary to meet this minimum gross weight; the

study airplane as illustrated in figure 2 has a wing area of 12 677 ft^2 and four 100 000-lb-thrust engines. A highly blended and integrated configuration such as the subject of this report requires a great deal of effort in the sizing process to maintain the desired configuration attributes. No reconfiguration of the concept was conducted to match the minimum gross weight sizing results.

Discussion of Results

An upper limit of acceptability for takeoff gross weight of large transport aircraft currently appears to exist near 1 000 000 lb. This ceiling is set by the interaction of many factors, only some of which are a function of the technology built into the airplane. Some are the result of airport physical limits such as runway and taxiway dimensions, pavement strength, and gate spacing among many others. The most significant of these "others" are environmentally motivated constraints such as community noise limits, exhaust emission limits, and sonic boom overpressure limits. Of these, only the latter problem is unique to the HSCT; significant technical challenges in these areas are also present for new subsonic transports.

The objective of the current study was to provide a baseline from which to assess the impact of changes in technology or changes in operational constraints. As such, it was unconstrained with respect to community noise, exhaust emissions, and sonic boom overpressure and assumed a technology level representative of the year 2015. Given the high weight sensitivity of long-range aircraft (i.e., the gross weight change resulting from changes in fuel weight or empty weight) it is likely that the current study configuration would weigh far in excess of 1 000 000 lb before meeting current noise and sonic boom criteria, assuming that closure on a design could even be obtained. It appears unlikely that limits on noise, emissions, and sonic boom will relax, or indeed even remain at current levels, in the near future. Therefore, *for the technology level assumed,* the study configuration would not be a viable HSCT concept. However, it is possible that a breakthrough in one or more major technology areas could change this conclusion and form a basis for further development of the concept.

Concluding Remarks

A Mach 4 high-speed civil transport (HSCT) concept was developed as part of a national program directed at identifying the technologies that may enable a viable long-range HSCT system. The study aircraft was a derivative of a previously developed Mach 3 concept and was developed without the constraints of community noise or sonic boom limits in order to provide a baseline from which to assess the effect of these constraints in further studies.

The concept was configured to carry 250 passengers for 6500 n. mi. with reserves. The propulsion, structures, and materials technologies used in the analysis of the concept assumed a technology availability date of 2015. The airplane was highly blended to achieve efficient volume utilization and high aerodynamic efficiency and used advanced, afterburning turbojet engines and a passive thermal management system. Advanced materials and fabrication techniques such as superplastically formed, diffusion-bonded (SPF/DB) titanium and graphite/polyimide composites were assumed for the airframe structure, and subsystems weight improvements of 15 to 20 percent relative to current practice were assumed. Estimated maximum trimmed lift-drag ratios of the configuration varied from 13.7 at high subsonic speed to 7.3 at the Mach 4 design point.

The minimum gross weight airplane capable of meeting the design mission performance requirements was estimated to weigh 865 700 lb. It had a wing area of 12 700 ft^2 and four engines rated at 111 000 lb thrust each. While an airplane of this size and weight is a marginally acceptable candidate to fit into the existing world airport infrastructure, it is apparent that the inclusion of additional constraints such as community noise and sonic boom limits would quickly cause the airplane to grow beyond acceptable size and weight limits with the technology levels assumed in this study.

NASA Langley Research Center
Hampton, VA 23665-5225
October 17, 1990

References

1. *National Aeronautical R&D Goals—Agenda for Achievement.* Executive Off. of the President, Off. of Science & Technology Policy, Feb. 1987.
2. Harris, Roy V., Jr.: On the Threshold—The Outlook for Supersonic and Hypersonic Aircraft. AIAA-89-2071, July–Aug. 1989.
3. Robins, A. Warner; Dollyhigh, Samuel M.; Beissner, Fred L., Jr.; Geiselhart, Karl; Martin, Glenn L.; Shields, E. W.; Swanson, E. E.; Coen, Peter G.; and Morris, Shelby J., Jr.: *Concept Development of a Mach 3.0 High-Speed Civil Transport.* NASA TM-4058, 1988.
4. New Airplane Development, Boeing Commercial Airplanes: *High-Speed Civil Transport Study.* NASA CR-4233, 1989.
5. Welge, H. Robert; and Graf, Donald A.: Vehicle Concept Design Considerations for Future High-Speed Commercial Flight. AIAA-87-2927, Sept. 1987.
6. Morris, Shelby J., Jr.; Strack, William C.; and Weidner, John P.: Propulsion System Issues for the High-Speed Civil Transport Study. AIAA-87-2938, Sept. 1987.

7. van Dam, C. P.: Swept Wing-Tip Shapes for Low-Speed Airplanes. *SAE Trans.*, Section 6, vol. 94, 1985, pp. 6.355–6.364.
8. van Dam, C. P.: Induced-Drag Characteristics of Crescent-Moon-Shaped Wings. *J. Aircr.*, vol. 24, no. 2, Feb. 1987, pp. 115–119.
9. Vijgen, P. M. H. W.; van Dam, C. P.; and Holmes, B. J.: Sheared Wing-Tip Aerodynamics: Wind-Tunnel and Computational Investigations of Induced-Drag Reduction. AIAA-87-2481 CP, Aug. 1987.
10. Naik, D. A.; and Ostowari, C.: An Experimental Study of the Aerodynamic Characteristics of Planar and Non-Planar Outboard Wing Planforms. AIAA-87-0588, Jan. 1987.
11. Rao, Dhanvada M.; and Johnson, Thomas D., Jr.: *Subsonic Pitch-Up Alleviation on a 74 Deg. Delta Wing.* NASA CR-165749, 1981.
12. Brandon, Jay M.; Murri, Daniel G.; and Nguyen, Luat T.: Experimental Study of Effects of Forebody Geometry on High Angle of Attack Static and Dynamic Stability and Control. *ICAS Proceedings—1986, 15th Congress of the International Council of the Aeronautical Sciences, Volume 1,* P. Santini and R. Staufenbiel, eds., American Inst. of Aeronautics and Astronautics, Inc., 1986, pp. 560–572. (Available as ICAS-86-5.4.1.)
13. Özişik, M. Necati: *Basic Heat Transfer.* McGraw-Hill, Inc., c.1977.
14. *SAE Aerospace Applied Thermodynamics Manual.* ARP 1168, Soc. of Automotive Engineers, Inc., c.1969.
15. Welty, James R.: *Engineering Heat Transfer—SI Version.* John Wiley & Sons, Inc., c.1978.
16. McCullers, L. A.:. Aircraft Configuration Optimization Including Optimized Flight Profiles. *Recent Experiences in Multidisciplinary Analysis and Optimization,* Jaroslow Sobieski, compiler, NASA CP-2327, Part 1, 1984, pp. 395–412.
17. Sommer, Simon C.; and Short, Barbara J.: *Free-Flight Measurements of Turbulent-Boundary-Layer Skin Friction in the Presence of Severe Aerodynamic Heating at Mach Numbers From 2.8 to 7.0.* NACA TN 3391, 1955.
18. *USAF Stability and Control Datcom.* Contracts AF33 (616)-6460 and F33615-76-C-3061, McDonnell Douglas Corp., Oct. 1960. (Revised Apr. 1978.)
19. Harris, Roy V., Jr.: *An Analysis and Correlation of Aircraft Wave Drag.* NASA TM X-947, 1964.
20. Craidon, Charlotte B.: *Description of a Digital Computer Program for Airplane Configuration Plots.* NASA TM X-2074, 1970.
21. Carlson, Harry W.; Mack, Robert J.; and Barger, Raymond L.: *Estimation of Attainable Leading-Edge Thrust for Wings at Subsonic and Supersonic Speeds.* NASA TP-1500, 1979.
22. Carlson, Harry W.; and Walkley, Kenneth B.: *An Aerodynamic Analysis Computer Program and Design Notes for Low Speed Wing Flap Systems.* NASA CR-3675, 1983.
23. Middleton, W. D.; and Lundry, J. L.: *A System for Aerodynamic Design and Analysis of Supersonic Aircraft. Part 1—General Description and Theoretical Development.* NASA CR-3351, 1980.
24. Middleton, W. D.; Lundry, J. L.; and Coleman, R. G.: *A System for Aerodynamic Design and Analysis of Supersonic Aircraft. Part 2—User's Manual.* NASA CR-3352, 1980.
25. Middleton, W. D.; and Lundry, J. L.: *A System for Aerodynamic Design and Analysis of Supersonic Aircraft. Part 4—Test Cases.* NASA CR-3354, 1980.
26. Fishbach, Laurence H.; and Caddy, Michael J.: *NNEP—The Navy NASA Engine Program.* NASA TM X-71857, 1975.
27. Morris, Shelby J., Jr.; Nelms, Walter P., Jr.; and Bailey, Rodney O.: *A Simplified Analysis of Propulsion Installation Losses for Computerized Aircraft Design.* NASA TM X-73136, 1976.
28. Ball, W. H.: *Rapid Evaluation of Propulsion System Effects. Volume IV—Library of Configurations and Performance Maps.* AFFDL-TR-78-91, Vol. IV, U.S. Air Force, July 1978.

Table I. Configuration Geometry

Geometry	Wing	Vertical tail
Area, ft^2	12 677	325
Mean aerodynamic chord length, ft	145.37	24.96
Span, ft	153.0	14.76
Aspect ratio (reference)	3.039	0.67
Taper ratio (reference)	0.235	0.225
LE sweep, deg	80, 53	69
Root t/c, percent	2.319	2.500
Break t/c, percent	3.148	
Tip t/c, percent	2.250	

Table II. Mass and Balance Summary

Component	Weight, lb	FS c.g., in.
Wing	64 280	1821
Vertical tail	3 171	3473
Fuselage	54 763	1860
Landing gear	26 508	1802
Nacelles	29 503	2093
Structure total	178 226	1904
Engines	28 652	2502
Miscellaneous systems	2 180	1566
Fuel system	7 115	1891
Propulsion total	37 947	2334
Surface controls	9 263	2006
Auxiliary power	1 847	3350
Instruments	2 911	1204
Hydraulics	7 770	1913
Electrical	3 333	1328
Avionics	1 546	720
Furnishings and equipment	23 776	1898
Air conditioning	7 278	1960
Anti-icing	173	2002
Additional thermal protection	14 342	1889
Systems and equipment total	72 239	1930
Weight empty	288 412	1954
Crew and baggage – Flight, 2	450	630
– Cabin, 7	1 130	1898
Unusable fuel	2 788	1891
Engine oil	944	2502
Passenger service	3 350	1782
Operating weight empty	297 074	1951
Passengers (251)	41 415	1782
Passenger baggage	11 044	1900
Miscellaneous items	2 575	1860
Zero fuel weight	352 108	1929
Mission fuel (maximum)	635 980	1683
Ramp weight (maximum)	988 088	1771

Table III. Numerical Model for Zero-Lift Drag Analysis

```
2AST4B-2 WAVE DRAG MODEL
  1  1 -1  1  1        17 20  2 20 30 20  3              2 10  1 10
12677.0                                                              REFA
  0.000  0.500  0.750  1.250  2.500  5.000  7.500 10.000 15.000 20.000 XAF 1
 25.000 30.000 35.000 40.000 50.000 60.000 70.000 80.000 90.000100.000 XAF 2
 11.517  7.650 -4.100201.821                                         WORG 4
 23.539 10.200 -5.100189.791                                         WORG 5
 38.000 12.750 -6.100175.329                                         WORG 6
 52.462 15.300 -6.900160.868                                         WORG 7
 66.923 17.850 -7.600146.407                                         WORG 8
 81.385 20.400 -8.300131.945                                         WORG 9
 95.847 22.950 -8.825118.690                                         WORG10
110.309 25.500 -9.275105.435                                         WORG11
124.770 28.050 -9.675 92.181                                         WORG12
139.232 30.600 -9.900 78.927                                         WORG13
153.694 33.150-10.077 65.672                                         WORG14
163.540 34.886-10.050 56.415                                         WORG15
174.760 40.800 -9.180 48.227                                         WORG16
192.440 54.060 -7.619 37.459                                         WORG17
214.705 69.360 -6.950 25.653                                         WORG18
224.031 73.440 -7.038 21.746                                         WORG19
243.168 76.806 -7.140  8.568                                         WORG20
    0.  -.056  -.085  -.146  -.313  -.625 -0.950 -1.250 -1.875 -2.450 ZORD 4-1
 -3.050 -3.670 -4.270 -4.900 -6.030 -7.090 -8.120 -9.100 -10.03 -10.80 ZORD 4-2
    0.  -.013  -.020  -.038  -.095  -.277  -.529  -.827 -1.464 -2.025 ZORD 5-1
 -2.550 -3.050 -3.600 -4.250 -5.200 -6.230 -7.210 -8.210 -9.180 -9.950 ZORD 5-2
    0.   .029   .042   .065   .107   .122   .023  -.129  -.520 -1.020 ZORD 6-1
 -1.533 -2.064 -2.596 -3.075 -4.200 -5.300 -6.380 -7.420 -8.460 -9.400 ZORD 6-2
    0.   .038   .055   .088   .155   .227   .198   .102  -.170  -.579 ZORD 7-1
 -1.015 -1.477 -1.961 -2.454 -3.410 -4.360 -6.310 -7.340 -7.490 -8.650 ZORD 7-2
    0.   .039   .057   .091   .164   .256   .267   .202  -.003  -.330 ZORD 8-1
  -.707 -1.107 -1.533 -1.976 -2.790 -3.670 -4.680 -5.760 -6.970 -8.350 ZORD 8-2
    0.   .036   .053   .087   .161   .282   .350   .343   .229   .026 ZORD 9-1
  -.233  -.562  -.894 -1.253 -2.050 -2.870 -3.760 -4.580 -5.550 -6.700 ZORD 9-2
    0.   .029   .042   .070   .136   .275   .380   .428   .368   .253 ZORD10-1
   .051  -.187  -.444  -.729 -1.350 -2.000 -2.650 -3.380 -4.150 -5.100 ZORD10-2
    0.   .028   .042   .069   .133   .257   .364   .429   .427   .356 ZORD11-1
   .230   .052  -.151  -.370  -.860 -1.410 -1.980 -2.550 -3.200 -3.920 ZORD11-2
    0.   .027   .040   .066   .127   .240   .342   .417   .470   .440 ZORD12-1
   .374   .260   .117  -.045  -.390  -.795 -1.200 -1.650 -2.180 -2.750 ZORD12-2
    0.   .025   .037   .061   .118   .221   .312   .389   .490   .500 ZORD13-1
   .476   .430   .356   .244  -.080  -.350  -.650  -.980 -1.280 -1.600 ZORD13-2
    0.   .017   .025   .041   .081   .157   .229   .297   .424   .505 ZORD14-1
   .557   .591   .610   .609   .500   .425   .300   .175   .025  -.125 ZORD14-2
    0.   .012   .018   .030   .060   .120   .182   .245   .386   .507 ZORD15-1
   .560   .600   .610   .609   .500 0.425 0.300 0.175 0.025  -.125 ZORD15-2
    0.  -.016  -.024  -.039  -.076  -.145  -.207  -.259  -.336  -.399 ZORD16-1
  -.452  -.492  -.523  -.551  -.593  -.624  -.649  -.666  -.683  -.770 ZORD16-2
    0.  -.012  -.018  -.031  -.061  -.120  -.176  -.231  -.332  -.422 ZORD17-1
  -.509  -.550  -.668  -.740  -.873  -.988 -1.086 -1.170 -1.232 -1.269 ZORD17-2
    0.  -.004  -.007  -.011  -.022  -.043  -.064  -.084  -.121  -.155 ZORD18-1
  -.184  -.212  -.237  -.261  -.301  -.342  -.388  -.426  -.459  -.494 ZORD18-2
    0.  -.002  -.003  -.005  -.009  -.019  -.027  -.036  -.052  -.067 ZORD19-1
  -.081  -.094  -.106  -.118  -.138  -.162  -.177  -.183  -.179  -.165 ZORD19-2
    0.  -.003  -.001  -.001  -.002  -.003  -.005  -.006  -.008  -.009 ZORD20-1
  -.010  -.011  -.011  -.010  -.007  -.002   .006   .015   .027   .041 ZORD20-2
```

Table III. Concluded

0.0000	0.1920	0.2280	0.2850	0.3830	0.5125	0.6113	0.6928	0.8222	0.9225	WORD 4-1
1.0001	1.0618	1.1076	1.1386	1.1594	1.1202	1.0025	0.7464	0.3611	0.0000	WORD 4-2
0.0000	0.1960	0.2325	0.2915	0.3950	0.5277	0.6296	0.7136	0.8469	0.9502	WORD 5-1
1.0311	1.0938	1.1410	1.1730	1.1944	1.1540	1.0324	0.7677	0.3712	0.0000	WORD 5-2
0.0000	0.2020	0.2410	0.3025	0.4070	0.5450	0.6504	0.7373	0.8751	0.9820	WORD 6-1
1.0655	1.1304	1.1792	1.2122	1.2344	1.1925	1.0666	0.7920	0.3828	0.0000	WORD 6-2
0.0000	0.2100	0.2505	0.3130	0.4215	0.5647	0.6739	0.7640	0.9069	1.0176	WORD 7-1
1.1043	1.1715	1.2221	1.2564	1.2794	1.2359	1.1050	0.8194	0.3959	0.0000	WORD 7-2
0.0000	0.2165	0.2580	0.3245	0.4365	0.5842	0.6974	0.7906	0.9386	1.0533	WORD 8-1
1.1430	1.2127	1.2651	1.3006	1.3243	1.2793	1.1434	0.8468	0.4089	0.0000	WORD 8-2
0.0000	0.2240	0.2675	0.3365	0.4545	0.5529	0.7260	0.8232	0.9775	1.0969	WORD 9-1
1.1904	1.2630	1.3176	1.3546	1.3793	1.3323	1.1904	0.8802	0.4249	0.0000	WORD 9-2
0.0000	0.2340	0.2800	0.3515	0.4730	0.6342	0.7573	0.8588	1.0198	1.1445	WORD10-1
1.2421	1.3178	1.3748	1.4134	1.4393	1.3902	1.2417	0.9167	0.4423	0.0000	WORD10-2
0.0000	0.2425	0.2890	0.3625	0.4870	0.6538	0.7329	0.8855	1.0516	1.1802	WORD11-1
1.2808	1.3590	1.4178	1.4576	1.4843	1.4335	1.2801	0.9441	0.4553	0.0000	WORD11-2
0.0000	0.2460	0.2955	0.3720	0.5010	0.6712	0.8017	0.9092	1.0798	1.2119	WORD12-1
1.3153	1.3956	1.4560	1.4969	1.5242	1.4721	1.3143	1.0134	0.4669	0.0000	WORD12-2
0.0000	0.2510	0.3015	0.3770	0.5075	0.6821	0.8147	0.9240	1.0974	1.2317	WORD13-1
1.3368	1.4184	1.4798	1.5214	1.5492	1.4962	1.3357	0.9836	0.4742	0.0000	WORD13-2
0.0000	0.2555	0.3050	0.3820	0.5130	0.6886	0.8225	0.9329	1.0801	1.2436	WORD14-1
1.3497	1.4321	1.4941	1.5361	1.5642	1.5107	1.3485	0.9927	0.4785	0.0000	WORD14-2
0.0000	0.2575	0.3080	0.3860	0.5160	0.6930	0.8277	0.9388	1.1151	1.2516	WORD15-1
1.3583	1.4413	1.5037	1.5459	1.5742	1.5203	1.3570	0.9988	0.4814	0.0000	WORD15-2
0.0000	0.2370	0.2920	0.3710	0.4990	0.6712	0.8017	0.9092	1.0798	1.2119	WORD16-1
1.3153	1.3956	1.4560	1.4969	1.5242	1.4721	1.3143	0.9684	0.4669	0.0000	WORD16-2
0.0000	0.1920	0.2414	0.3110	0.4240	0.5668	0.6765	0.7669	0.9104	1.0216	WORD17-1
1.1086	1.1761	1.2269	1.2613	1.2843	1.2407	1.1093	0.8224	0.3973	0.0000	WORD17-2
0.0000	0.1775	0.2230	0.2825	0.3820	0.5103	0.6087	0.6899	0.8187	0.9185	WORD18-1
0.9966	1.0572	1.1028	1.1337	1.1544	1.1154	0.9982	0.7434	0.3596	0.0000	WORD18-2
0.0000	0.1724	0.2175	0.2767	0.3745	0.5428	0.5983	0.6780	0.8046	0.9027	WORD19-1
0.9794	1.0389	1.0837	1.1141	1.1344	1.0961	0.9811	0.7312	0.3538	0.0000	WORD19-2
0.0000	0.1718	0.2166	0.2702	0.3711	0.4973	0.5930	0.6721	0.7975	0.8947	WORD20-1
0.9708	1.0298	1.0742	1.1043	1.1244	1.0865	0.9726	0.7251	0.3509	0.0000	WORD20-2
0.	10.	20.	30.	40.	50.	60.	70.	80.	90.	XFUS1-1
100.	110.	120.	130.	140.	150.	160.	170.	180.	190.	XFUS1-2
200.	210.	220.	230.	240.	250.	260.	270.	280.	290.	XFUS1-3
0.	-.65	-1.3	-1.945	-2.568	-3.18	-3.76	-4.33	-4.845	-5.34	ZFUS1-1
-5.776	-6.163	-6.5	-6.775	-6.995	-7.165	-7.29	-7.375	-7.44	-7.48	ZFUS1-2
-7.495	-7.5	-7.455	-7.345	-7.145	-6.84	-6.447	-5.955	-5.345	-4.52	ZFUS1-3
0.	26.57	45.	61.78	74.04	85.14	97.3	105.62	112.13	120.92	AFUS1-1
127.06	135.03	142.56	151.62	159.4	163.56	166.99	169.1	168.17	162.15	AFUS1-2
152.64	139.47	124.52	106.29	86.59	66.72	47.89	31.84	18.22	8.3	AFUS1-3
290.01	300.	310.								XFUS2-1
-4.52	-3.43	-2.								ZFUS2-1
8.3	2.1	0.								AFUS2-1
157.88	9.92	-20.00								PORG 1
0.00	6.720	13.440	20.160	26.880	33.600	42.000	50.400	58.800	67.200	XPOD 1
4.460	4.585	4.710	4.835	4.960	4.860	4.760	4.660	4.560	4.460	PODR 1
157.88	19.84	-19.25								PORG 2
0.00	6.720	13.440	20.160	26.880	33.600	42.000	50.400	58.800	67.200	XPOD 2
4.460	4.585	4.710	4.835	4.960	4.860	4.760	4.660	4.560	4.460	PODR 2
261.4	0.0	-2.0	36.0	300.0	0.0	12.8	8.1			FORG 1
0.00	0.50	1.00	5.00	10.00	25.00	50.00	75.00	95.00	100.00	XFIN 1
0.00	0.03	0.05	0.26	0.50	1.13	1.50	1.12	0.26	0.00	FORD 1

Table IV. Numerical Model for Analysis at Lift

```
2AST4B-2 ANLZ MODEL
  1  1  0  1  0        20 20  0 00 00 00  0                2 10  0 00
12677.0 145.37  150.0                                                  SCAXR
  0.000  0.500  0.750  1.250  2.500  5.000  7.500 10.000 15.000 20.000 XAF 1
 25.000 30.000 35.000 40.000 50.000 60.000 70.000 80.000 90.000100.000 XAF 2
  0.000  0.000 -1.300310.000                                           WORG 1
  3.506  2.550 -2.492274.710                                           WORG 2
  7.403  5.100 -3.975234.389                                           WORG 3
 11.517  7.650 -4.100201.821                                           WORG 4
 23.539 10.200 -5.100189.791                                           WORG 5
 38.000 12.750 -6.100175.329                                           WORG 6
 52.462 15.300 -6.900160.868                                           WORG 7
 66.923 17.850 -7.600146.407                                           WORG 8
 81.385 20.400 -8.300131.945                                           WORG 9
 95.847 22.950 -8.825118.690                                           WORG10
110.309 25.500 -9.275105.435                                           WORG11
124.770 28.050 -9.675 92.181                                           WORG12
139.232 30.600 -9.900 78.927                                           WORG13
153.694 33.150-10.077 65.672                                           WORG14
163.540 34.886-10.050 56.415                                           WORG15
174.760 40.800 -9.180 48.227                                           WORG16
192.440 54.060 -7.619 37.459                                           WORG17
214.705 69.360 -6.950 25.653                                           WORG18
224.031 73.440 -7.038 21.746                                           WORG19
243.168 76.806 -7.140  8.568                                           WORG20
  0.000 -0.103 -0.154 -0.257 -0.513 -1.020 -1.514 -2.006 -2.981 -3.898 ZORD 1-1
 -4.735 -5.476 -6.100 -6.600 -7.242 -7.502 -7.439 -6.915 -5.406 -1.990 ZORD 1-2
  0.000 -0.106 -0.159 -0.265 -0.524 -1.007 -1.406 -1.722 -2.211 -2.705 ZORD 2-1
 -3.259 -3.844 -4.495 -5.055 -5.624 -5.966 -6.101 -5.899 -5.240 -3.971 ZORD 2-2
  0.000 -0.087 -0.131 -0.218 -0.430 -0.820 -1.154 -1.455 -2.050 -2.662 ZORD 3-1
 -3.261 -3.822 -4.247 -4.489 -4.801 -5.064 -5.198 -5.123 -4.736 -4.031 ZORD 3-2
     0.  -.056  -.085  -.146  -.313  -.625 -0.950 -1.250 -1.875 -2.450 ZORD 4-1
 -3.050 -3.670 -4.270 -4.900 -6.030 -7.090 -8.120 -9.100 -10.03 -10.80 ZORD 4-2
     0.  -.013  -.020  -.038  -.095  -.277  -.529  -.827 -1.464 -2.025 ZORD 5-1
 -2.550 -3.050 -3.600 -4.250 -5.200 -6.230 -7.210 -8.210 -9.180 -9.950 ZORD 5-2
     0.   .029   .042   .065   .107   .122   .023  -.129  -.520 -1.020 ZORD 6-1
 -1.533 -2.064 -2.596 -3.075 -4.200 -5.300 -6.380 -7.420 -8.460 -9.400 ZORD 6-2
     0.   .038   .055   .088   .155   .227   .198   .102  -.170  -.579 ZORD 7-1
 -1.015 -1.477 -1.961 -2.454 -3.410 -4.360 -6.310 -7.340 -7.490 -8.650 ZORD 7-2
     0.   .039   .057   .091   .164   .256   .267   .202  -.003  -.330 ZORD 8-1
  -.707 -1.107 -1.533 -1.976 -2.790 -3.670 -4.680 -5.760 -6.970 -8.350 ZORD 8-2
     0.   .036   .053   .087   .161   .282   .350   .343   .229   .026 ZORD 9-1
  -.233  -.562  -.894 -1.253 -2.050 -2.870 -3.760 -4.580 -5.550 -6.700 ZORD 9-2
     0.   .029   .042   .070   .136   .275   .380   .428   .368   .253 ZORD10-1
   .051  -.187  -.444  -.729 -1.350 -2.000 -2.650 -3.380 -4.150 -5.100 ZORD10-2
     0.   .028   .042   .069   .133   .257   .364   .429   .427   .356 ZORD11-1
   .230   .052  -.151  -.370  -.860 -1.410 -1.980 -2.550 -3.200 -3.920 ZORD11-2
     0.   .027   .040   .066   .127   .240   .342   .417   .470   .440 ZORD12-1
   .374   .260   .117  -.045  -.390  -.795 -1.200 -1.650 -2.180 -2.750 ZORD12-2
     0.   .025   .037   .061   .118   .221   .312   .389   .490   .500 ZORD13-1
   .476   .430   .356   .244  -.080  -.350  -.650  -.980 -1.280 -1.600 ZORD13-2
     0.   .017   .025   .041   .081   .157   .229   .297   .424   .505 ZORD14-1
   .557   .591   .610   .609   .500   .425   .300   .175   .025  -.125 ZORD14-2
     0.   .012   .018   .030   .060   .120   .182   .245   .386   .507 ZORD15-1
   .560   .600   .610   .609   .500 0.425 0.300 0.175 0.025  -.125 ZORD15-2
     0.  -.016  -.024  -.039  -.076  -.145  -.207  -.259  -.336  -.399 ZORD16-1
  -.452  -.492  -.523  -.551  -.593  -.624  -.649  -.666  -.683  -.770 ZORD16-2
```

Table IV. Concluded

0.	-.012	-.018	-.031	-.061	-.120	-.176	-.231	-.332	-.422	ZORD17-1
-.509	-.550	-.668	-.740	-.873	-.988	-1.086	-1.170	-1.232	-1.269	ZORD17-2
0.	-.004	-.007	-.011	-.022	-.043	-.064	-.084	-.121	-.155	ZORD18-1
-.184	-.212	-.237	-.261	-.301	-.342	-.388	-.426	-.459	-.494	ZORD18-2
0.	-.002	-.003	-.005	-.009	-.019	-.027	-.036	-.052	-.067	ZORD19-1
-.081	-.094	-.106	-.118	-.138	-.162	-.177	-.183	-.179	-.165	ZORD19-2
0.	-.003	-.001	-.001	-.002	-.003	-.005	-.006	-.008	-.009	ZORD20-1
-.010	-.011	-.011	-.010	-.007	-.002	.006	.015	.027	.041	ZORD20-2
0.0000	0.0582	0.0873	0.1452	0.2876	0.5539	0.7780	0.9546	1.2165	1.4133	WORD 1-1
1.5711	1.7115	1.8471	1.9796	2.1979	2.2582	2.0578	1.5359	0.7946	0.0000	WORD 1-2
0.0000	0.0632	0.0947	0.1573	0.3100	0.5823	0.7884	0.9376	1.1527	1.3654	WORD 2-1
1.5786	1.7597	1.9151	2.0354	2.2132	2.3360	2.2918	2.0006	1.4099	0.0000	WORD 2-2
0.0000	0.0611	0.0915	0.1516	0.2949	0.5239	0.6624	0.7439	0.8771	1.0292	WORD 3-1
1.1600	1.2855	1.4328	1.6017	1.9222	2.1787	2.3079	2.2066	1.7025	0.0000	WORD 3-2
0.0000	0.1920	0.2280	0.2850	0.3830	0.5125	0.6113	0.6928	0.8222	0.9225	WORD 4-1
1.0001	1.0618	1.1076	1.1386	1.1594	1.1202	1.0025	0.7464	0.3611	0.0000	WORD 4-2
0.0000	0.1960	0.2325	0.2915	0.3950	0.5277	0.6296	0.7136	0.8469	0.9502	WORD 5-1
1.0311	1.0938	1.1410	1.1730	1.1944	1.1540	1.0324	0.7677	0.3712	0.0000	WORD 5-2
0.0000	0.2020	0.2410	0.3025	0.4070	0.5450	0.6504	0.7373	0.8751	0.9820	WORD 6-1
1.0655	1.1304	1.1792	1.2122	1.2344	1.1925	1.0666	0.7920	0.3828	0.0000	WORD 6-2
0.0000	0.2100	0.2505	0.3130	0.4215	0.5647	0.6739	0.7640	0.9069	1.0176	WORD 7-1
1.1043	1.1715	1.2221	1.2564	1.2794	1.2359	1.1050	0.8194	0.3959	0.0000	WORD 7-2
0.0000	0.2165	0.2580	0.3245	0.4365	0.5842	0.6974	0.7906	0.9386	1.0533	WORD 8-1
1.1430	1.2127	1.2651	1.3006	1.3243	1.2793	1.1434	0.8468	0.4089	0.0000	WORD 8-2
0.0000	0.2240	0.2675	0.3365	0.4545	0.5529	0.7260	0.8232	0.9775	1.0969	WORD 9-1
1.1904	1.2630	1.3176	1.3546	1.3793	1.3323	1.1904	0.8802	0.4249	0.0000	WORD 9-2
0.0000	0.2340	0.2800	0.3515	0.4730	0.6342	0.7573	0.8588	1.0198	1.1445	WORD10-1
1.2421	1.3178	1.3748	1.4134	1.4393	1.3902	1.2417	0.9167	0.4423	0.0000	WORD10-2
0.0000	0.2425	0.2890	0.3625	0.4870	0.6538	0.7329	0.8855	1.0516	1.1802	WORD11-1
1.2808	1.3590	1.4178	1.4576	1.4843	1.4335	1.2801	0.9441	0.4553	0.0000	WORD11-2
0.0000	0.2460	0.2955	0.3720	0.5010	0.6712	0.8017	0.9092	1.0798	1.2119	WORD12-1
1.3153	1.3956	1.4560	1.4969	1.5242	1.4721	1.3143	1.0134	0.4669	0.0000	WORD12-2
0.0000	0.2510	0.3015	0.3770	0.5075	0.6821	0.8147	0.9240	1.0974	1.2317	WORD13-1
1.3368	1.4184	1.4798	1.5214	1.5492	1.4962	1.3357	0.9836	0.4742	0.0000	WORD13-2
0.0000	0.2555	0.3050	0.3820	0.5130	0.6886	0.8225	0.9329	1.0801	1.2436	WORD14-1
1.3497	1.4321	1.4941	1.5361	1.5642	1.5107	1.3485	0.9927	0.4785	0.0000	WORD14-2
0.0000	0.2575	0.3080	0.3860	0.5160	0.6930	0.8277	0.9388	1.1151	1.2516	WORD15-1
1.3583	1.4413	1.5037	1.5459	1.5742	1.5203	1.3570	0.9988	0.4814	0.0000	WORD15-2
0.0000	0.2370	0.2920	0.3710	0.4990	0.6712	0.8017	0.9092	1.0798	1.2119	WORD16-1
1.3153	1.3956	1.4560	1.4969	1.5242	1.4721	1.3143	0.9684	0.4669	0.0000	WORD16-2
0.0000	0.1920	0.2414	0.3110	0.4240	0.5668	0.6765	0.7669	0.9104	1.0216	WORD17-1
1.1086	1.1761	1.2269	1.2613	1.2843	1.2407	1.1093	0.8224	0.3973	0.0000	WORD17-2
0.0000	0.1775	0.2230	0.2825	0.3820	0.5103	0.6087	0.6899	0.8187	0.9185	WORD18-1
0.9966	1.0572	1.1028	1.1337	1.1544	1.1154	0.9982	0.7434	0.3596	0.0000	WORD18-2
0.0000	0.1724	0.2175	0.2767	0.3745	0.5428	0.5983	0.6780	0.8046	0.9027	WORD19-1
0.9794	1.0389	1.0837	1.1141	1.1344	1.0961	0.9811	0.7312	0.3538	0.0000	WORD19-2
0.0000	0.1718	0.2166	0.2702	0.3711	0.4973	0.5930	0.6721	0.7975	0.8947	WORD20-1
0.9708	1.0298	1.0742	1.1043	1.1244	1.0865	0.9726	0.7251	0.3509	0.0000	WORD20-2
134.25	9.92	-20.00								PORG 1
0.00	9.083	18.167	27.250	36.333	45.417	54.500	63.583	81.750	90.833	XPOD 1
4.460	4.585	4.710	4.835	4.960	4.860	4.760	4.660	4.560	4.460	PODR 1
134.25	19.84	-19.25								PORG 2
0.00	9.083	18.167	27.250	36.333	45.417	54.500	63.583	81.750	90.833	XPOD 2
4.460	4.585	4.710	4.835	4.960	4.860	4.760	4.660	4.560	4.460	PODR 2

Table V. Primary Mission Performance Summary

Reference wing area, ft^2	12 700
Engine scale factor	3.801
Operating weight empty, lb	308 195
Payload, lb	55 034
Zero fuel weight, lb	363 229

Segment	Initial weight, lb	Fuel required, lb		Time, min		Distance, n. mi.		Mach number		Altitude	
		Segment	Total	Segment	Total	Segment	Total	Start	End	Start	End
Taxi out	865 658	4 926	4 926	10.0	10.0						
Takeoff	850 732	6 995	11 921	.4	10.4				0.3		0
Climb	853 737	84 258	96 179	13.5	23.9	205.9	205.9	0.3	4.0	0	80 946
Cruise	769 479	336 318	432 498	151.8	175.7	5891.6	6097.6	4.0	4.0	80 946	92 341
Descent	433 160	12 418	444 916	25.8	201.5	402.4	6500.0	4.0	0.3	92 341	0
Reserves	420 742	57 513	502 429								
Taxi in		2 463		5.0	206.5						

Design range, n. mi.	6 500
Flight time, hr	3.19
Block time, hr	3.44
Block fuel, lb	447 379

Table VI. Reserve Mission Details

Segment	Fuel burned, lb
Missed approach	1 921
Climb	10 873
Cruise ($M = 0.94$, $h = 43\,000$ ft)	4 901
Hold ($M = 0.8$, $h = 37\,000$ ft)	11 942
Descent	6 226
Subtotal	35 863
5 percent trip fuel ($0.05 \times 432\,994$)	21 650
Total	57 513

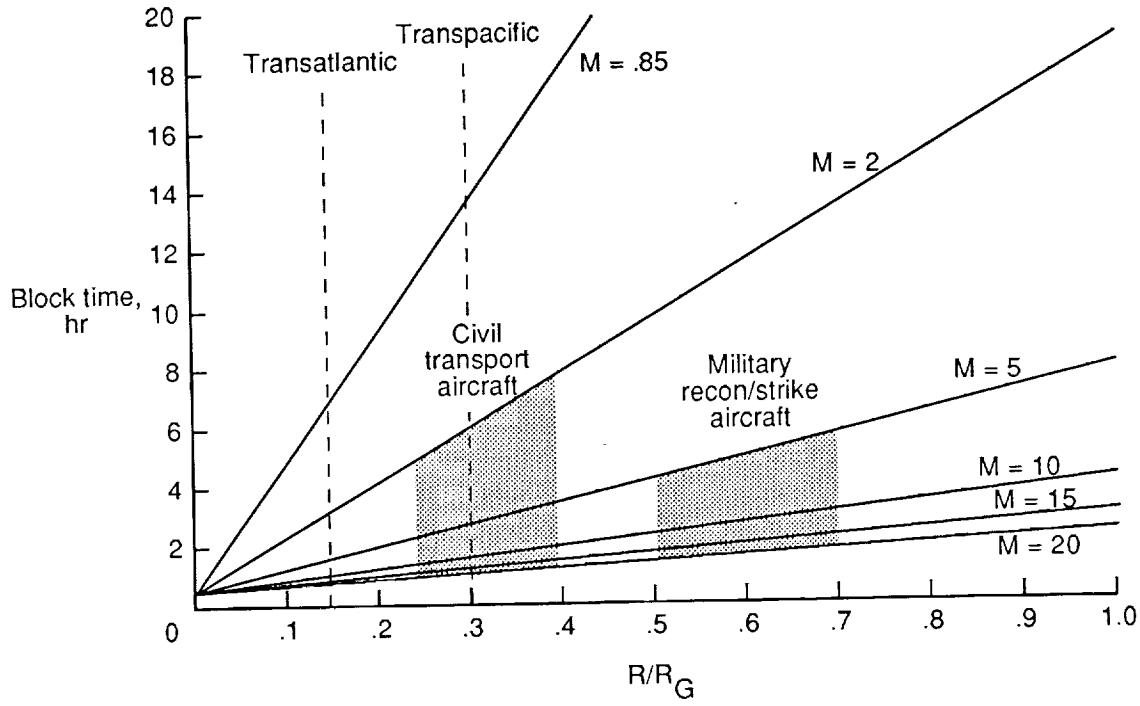

Figure 1. Block time for long-distance travel (ref. 2).

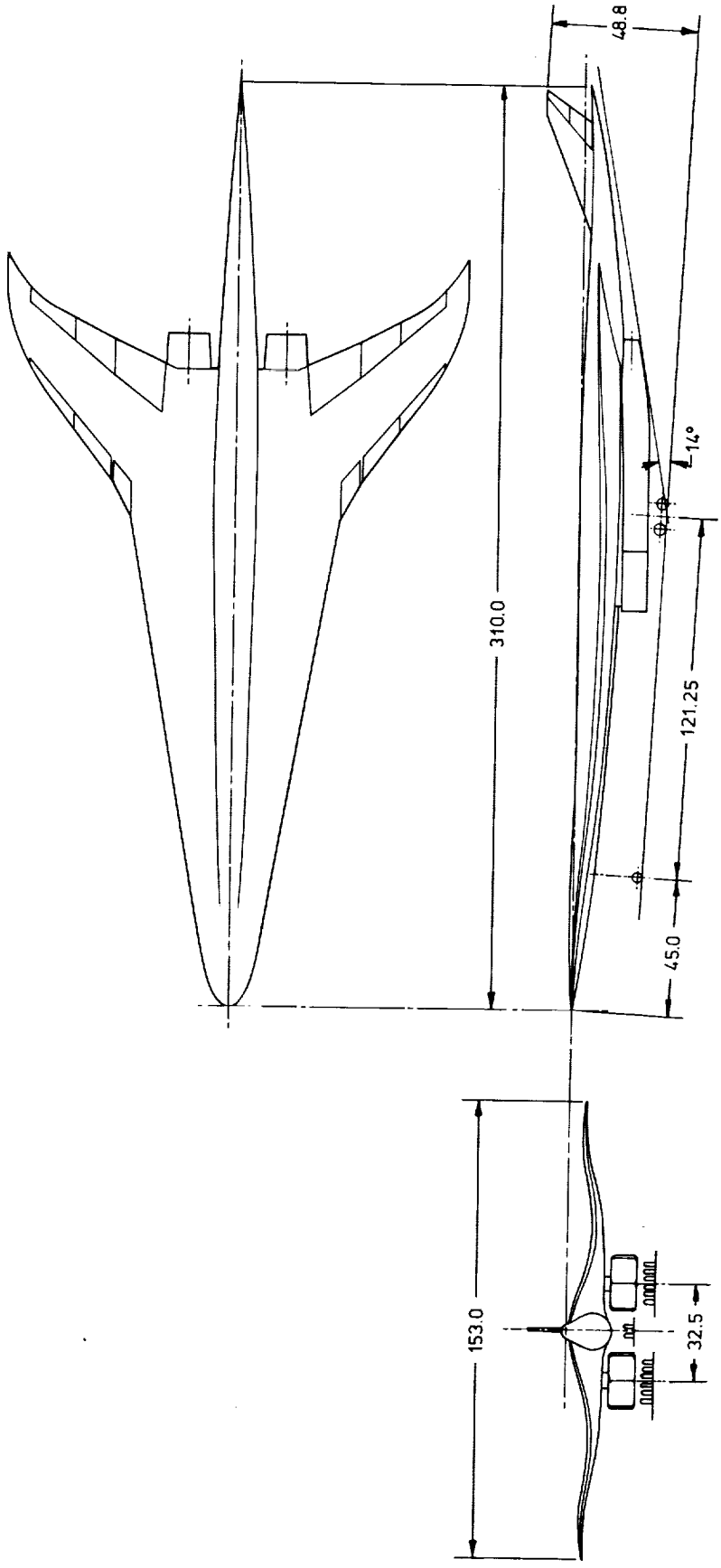

Figure 2. Study concept general arrangement. Dimensions in feet except as noted.

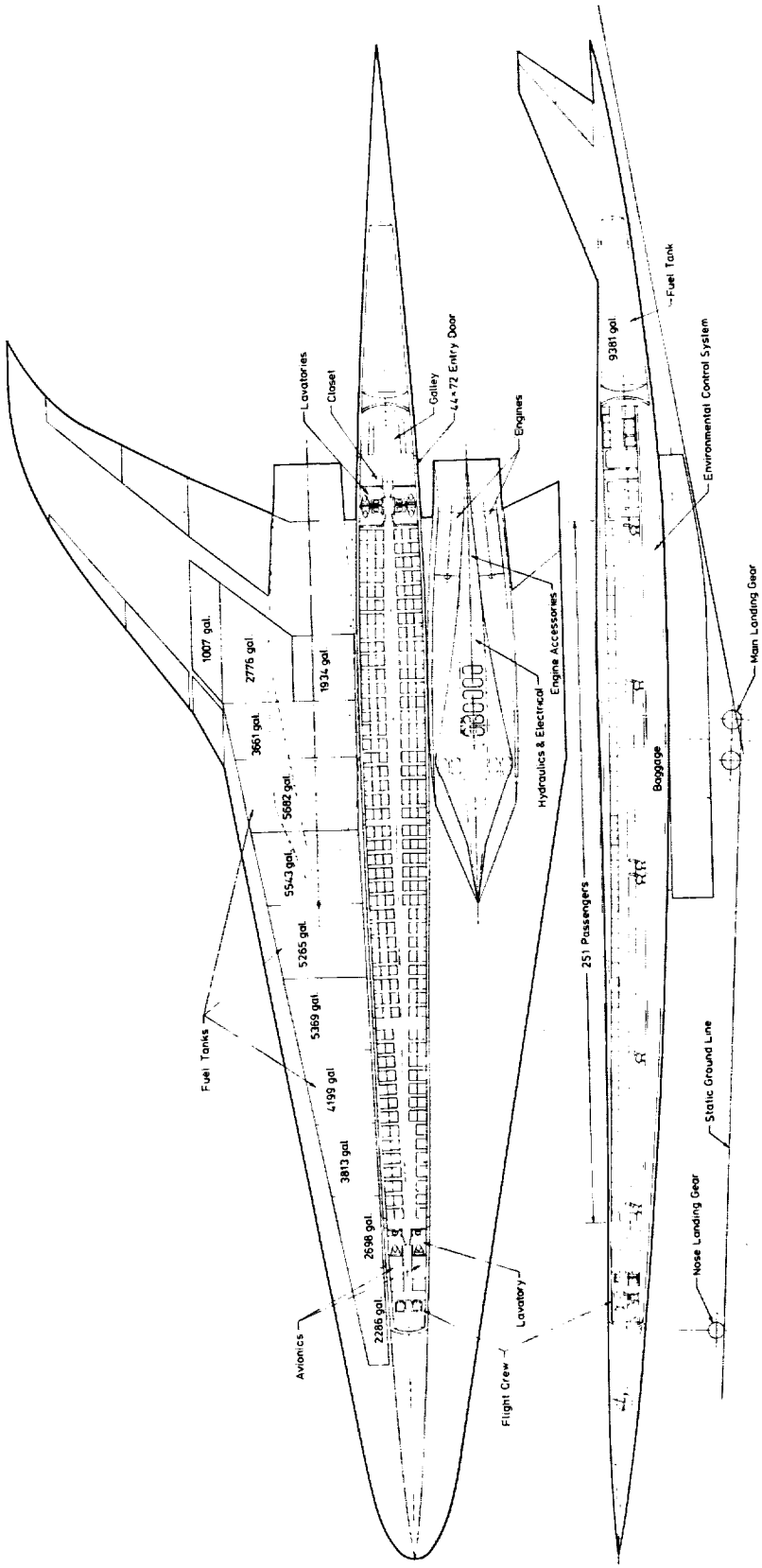

Figure 3. Study concept interior arrangement.

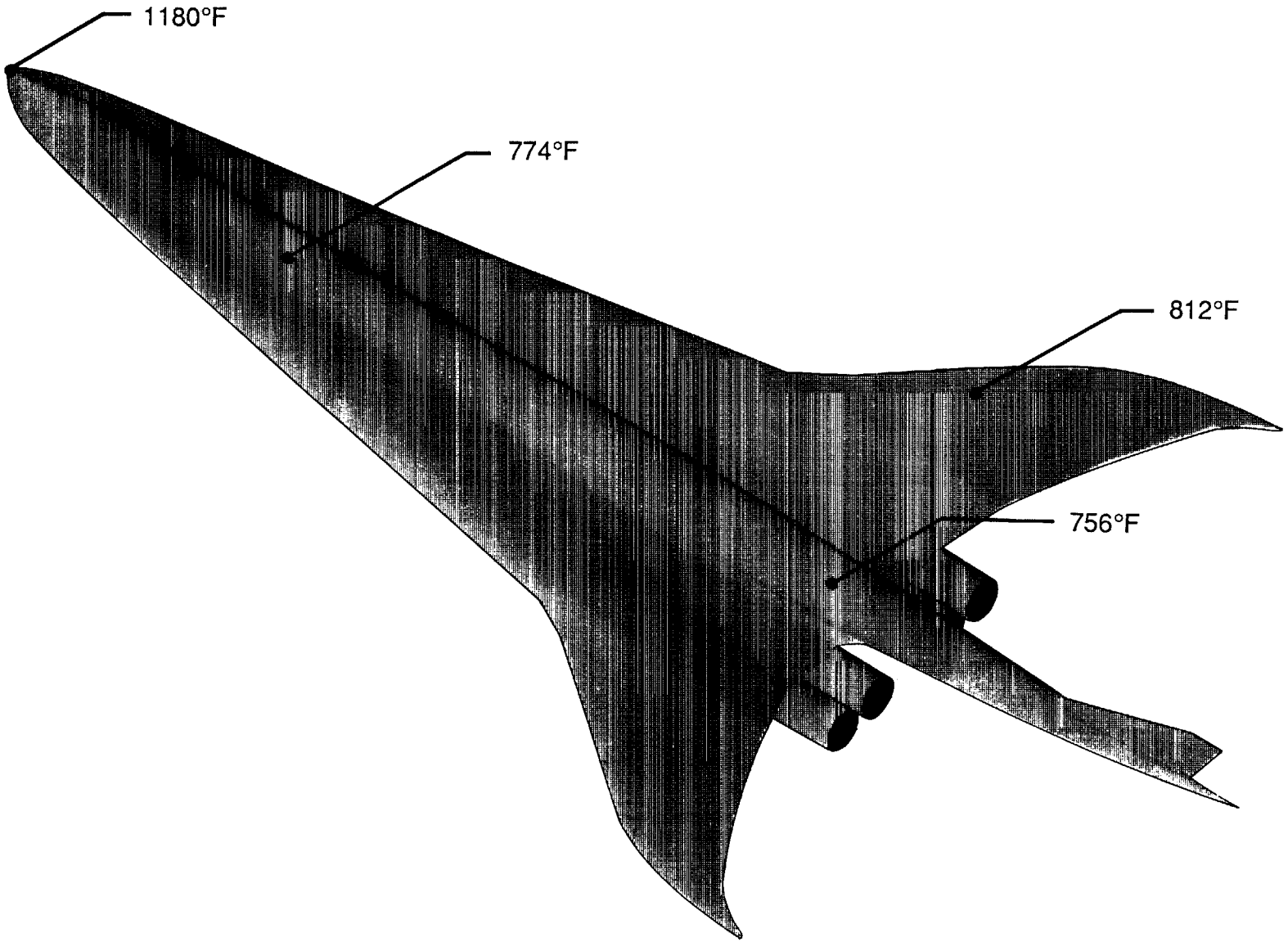

Figure 4. Estimated exterior skin temperatures at cruise.

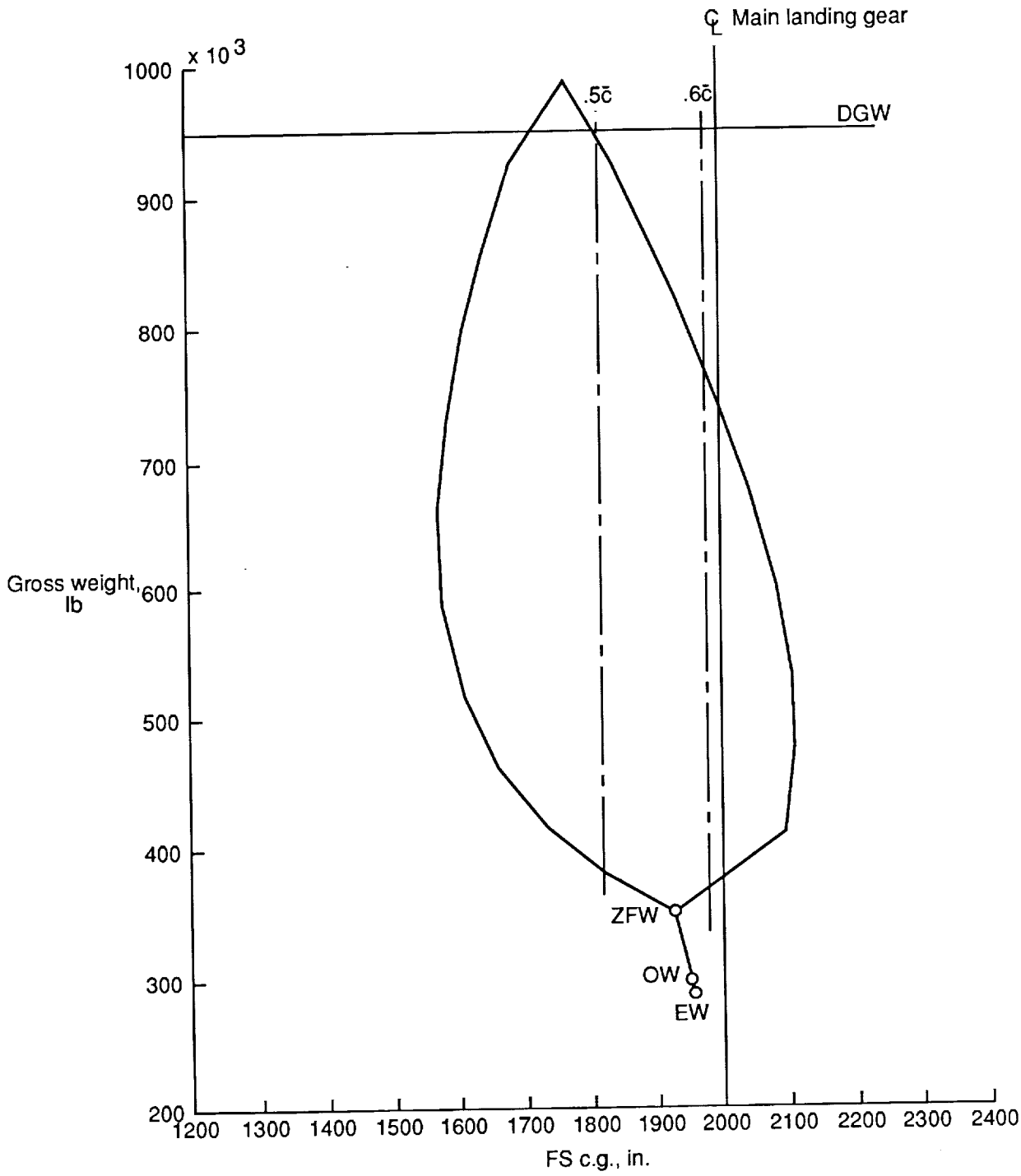

Figure 5. Study configuration center-of-gravity envelope.

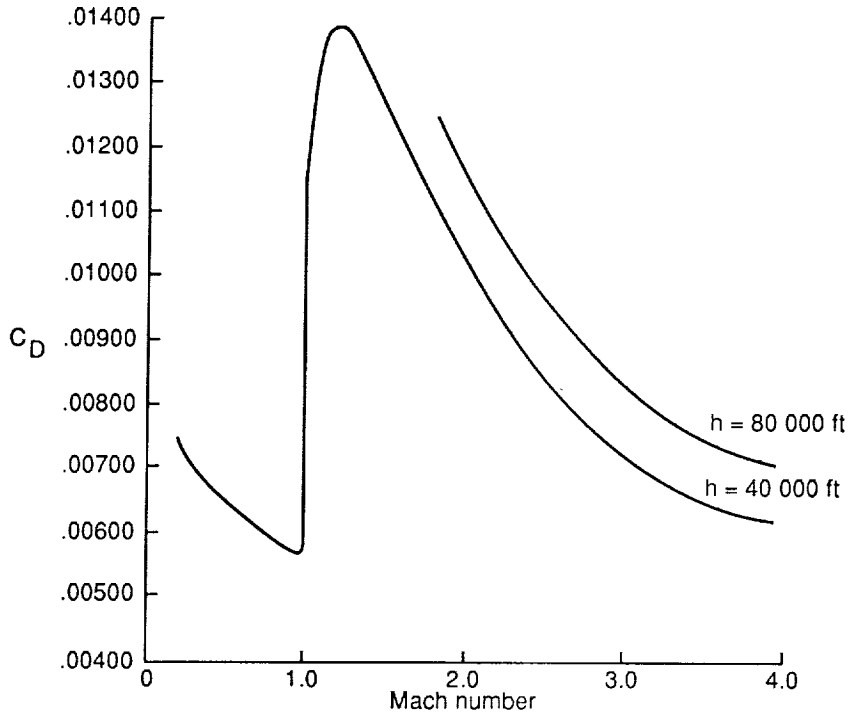

Figure 6. C_{D_0} characteristics. $S_{\text{ref}} = 12\,677$ ft^2.

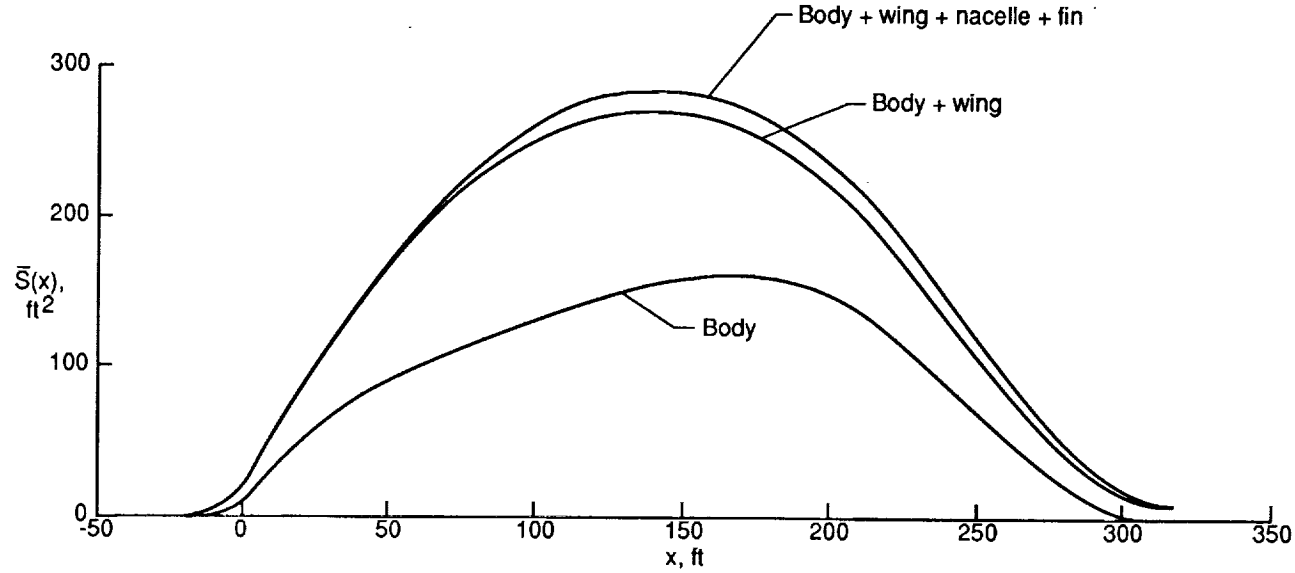

Figure 7. $M = 4$ average equivalent body areas.

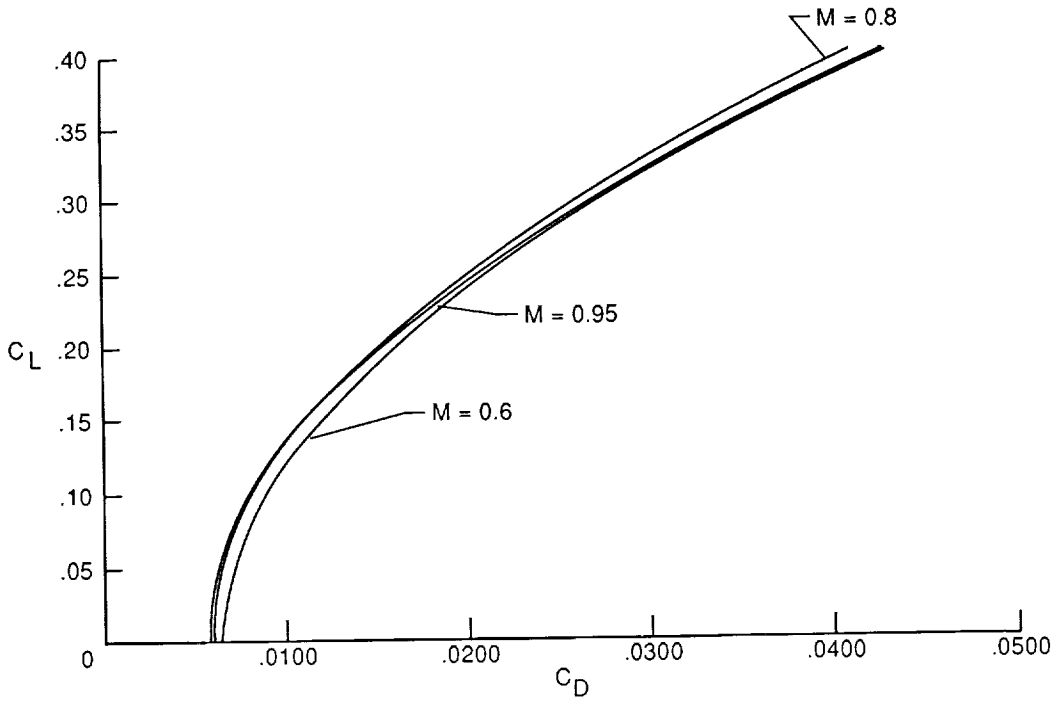

Figure 8. Subsonic drag polars. $S_{\text{ref}} = 12\,677$ ft^2.

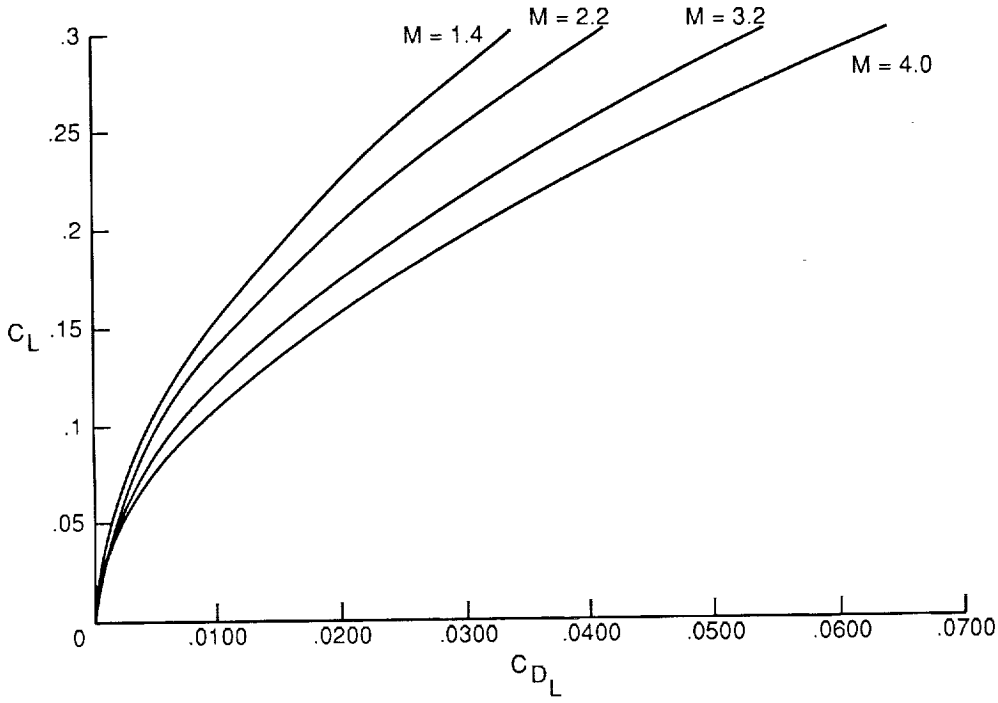

Figure 9. Predicted supersonic drag due to lift. $S_{\text{ref}} = 12\,677$ ft^2.

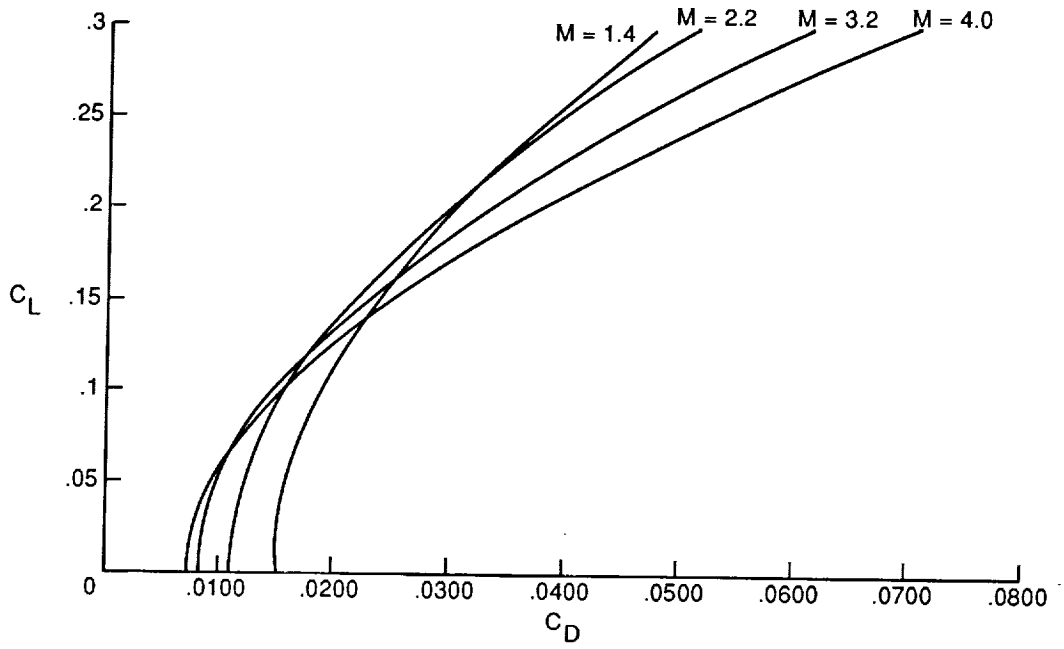

Figure 10. Supersonic total-drag polar at 80 000 ft. $S_{ref} = 12\,677$ ft^2.

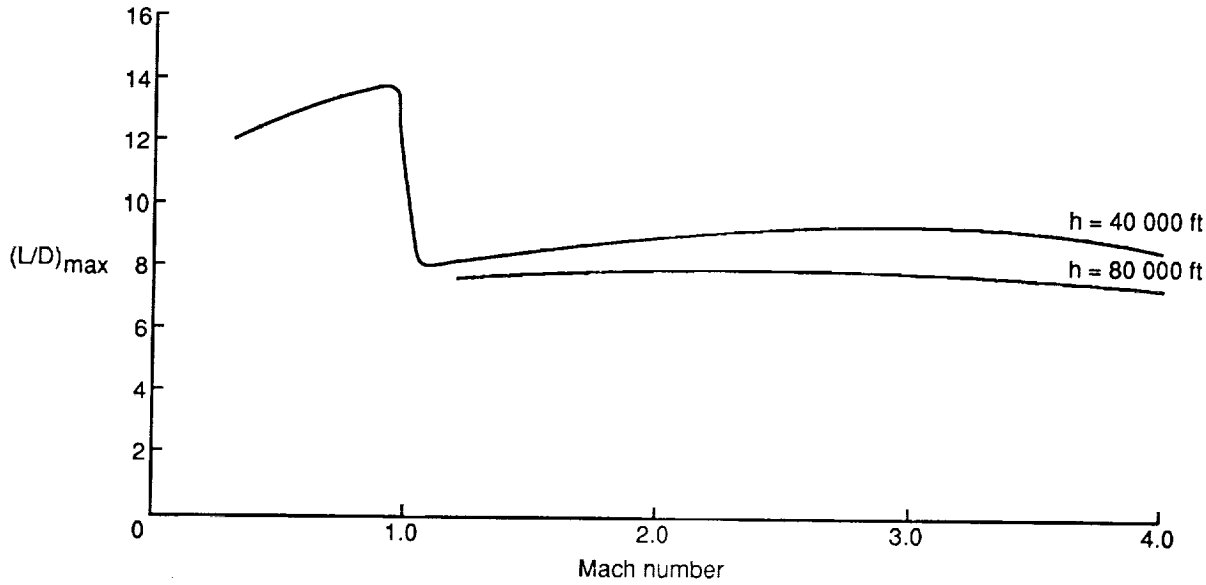

Figure 11. Study configuration maximum lift-drag ratios.

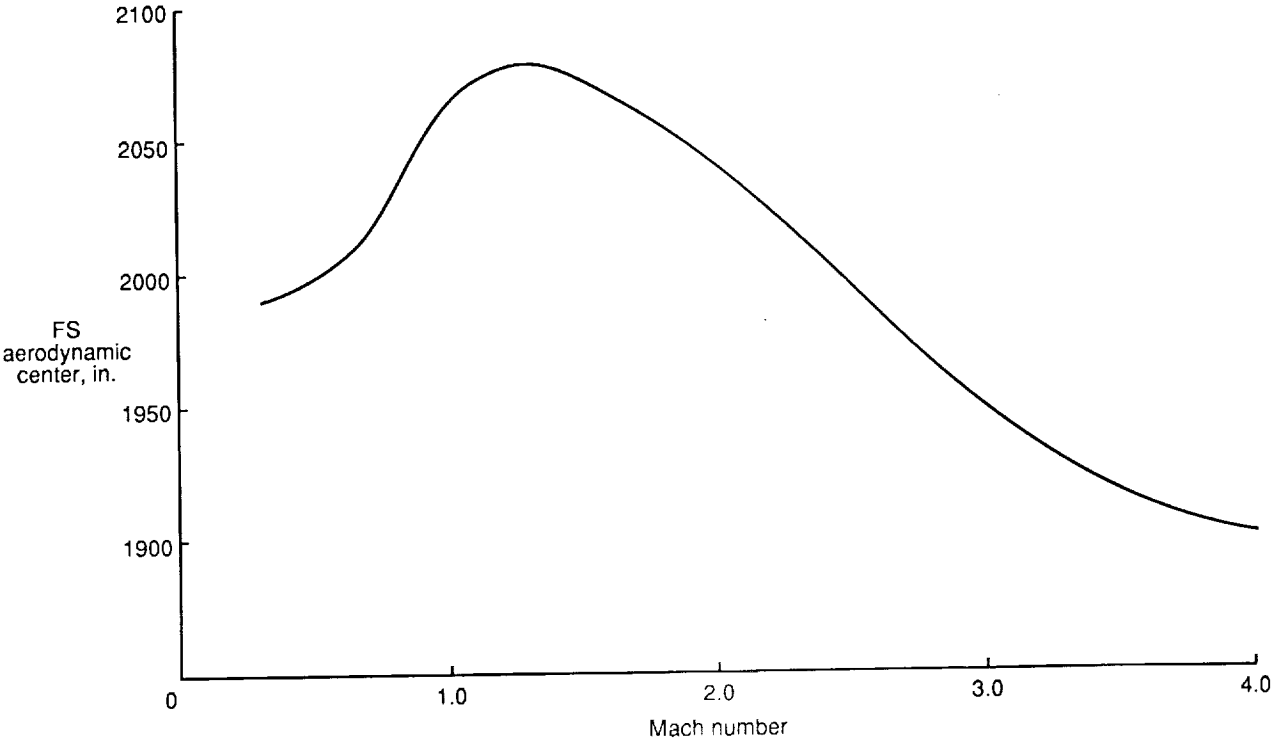

Figure 12. Aerodynamic center location.

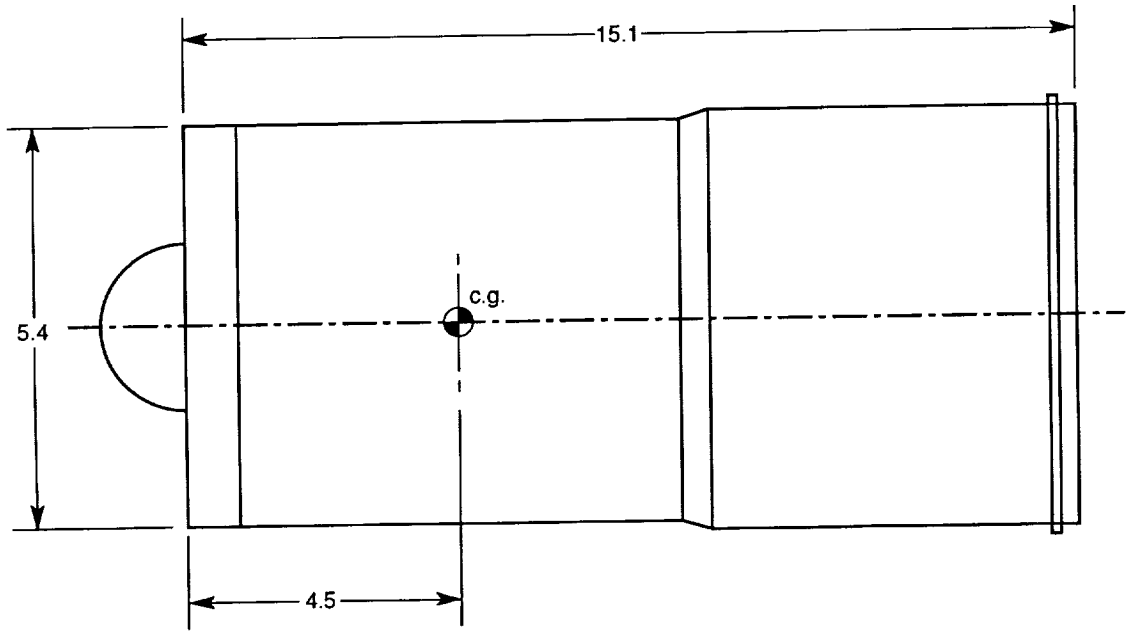

Figure 13. Engine geometry. Dimensions in feet.

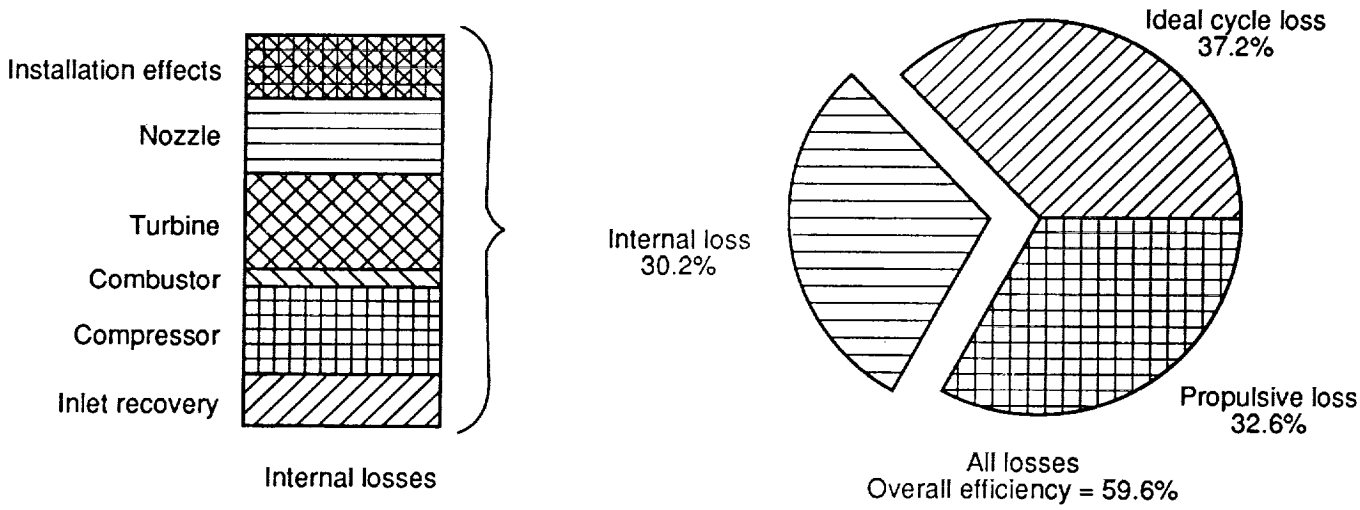

Figure 14. Propulsion system losses.

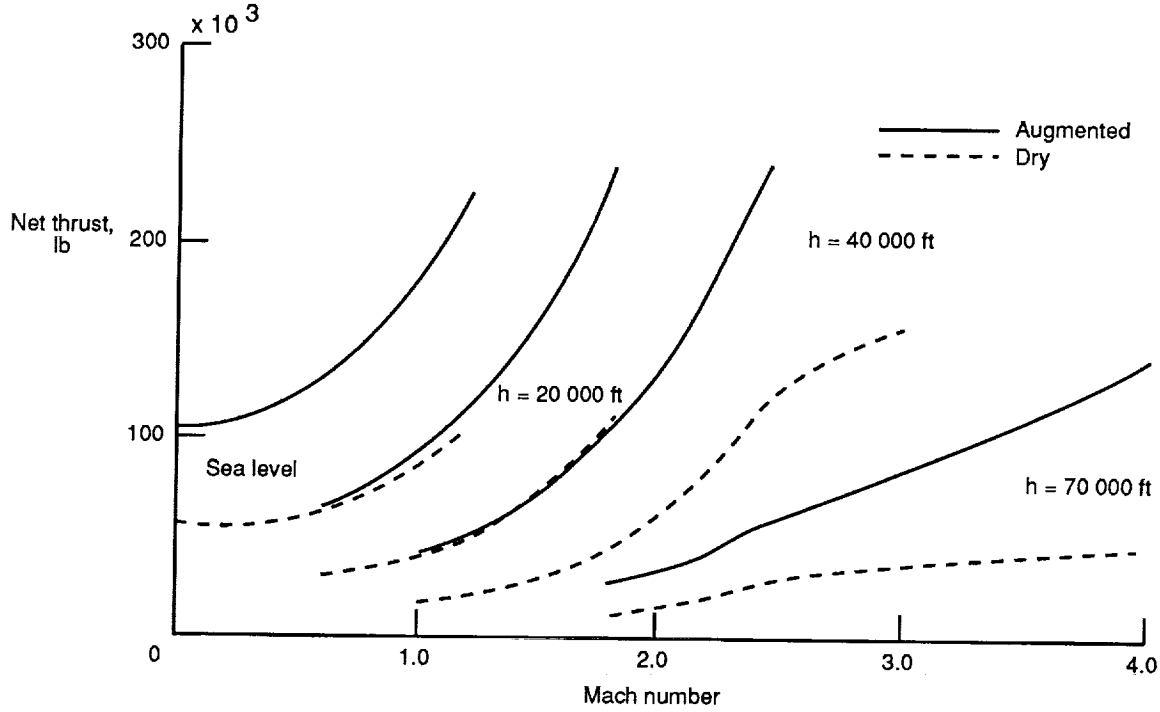

Figure 15. Installed engine thrust characteristics.

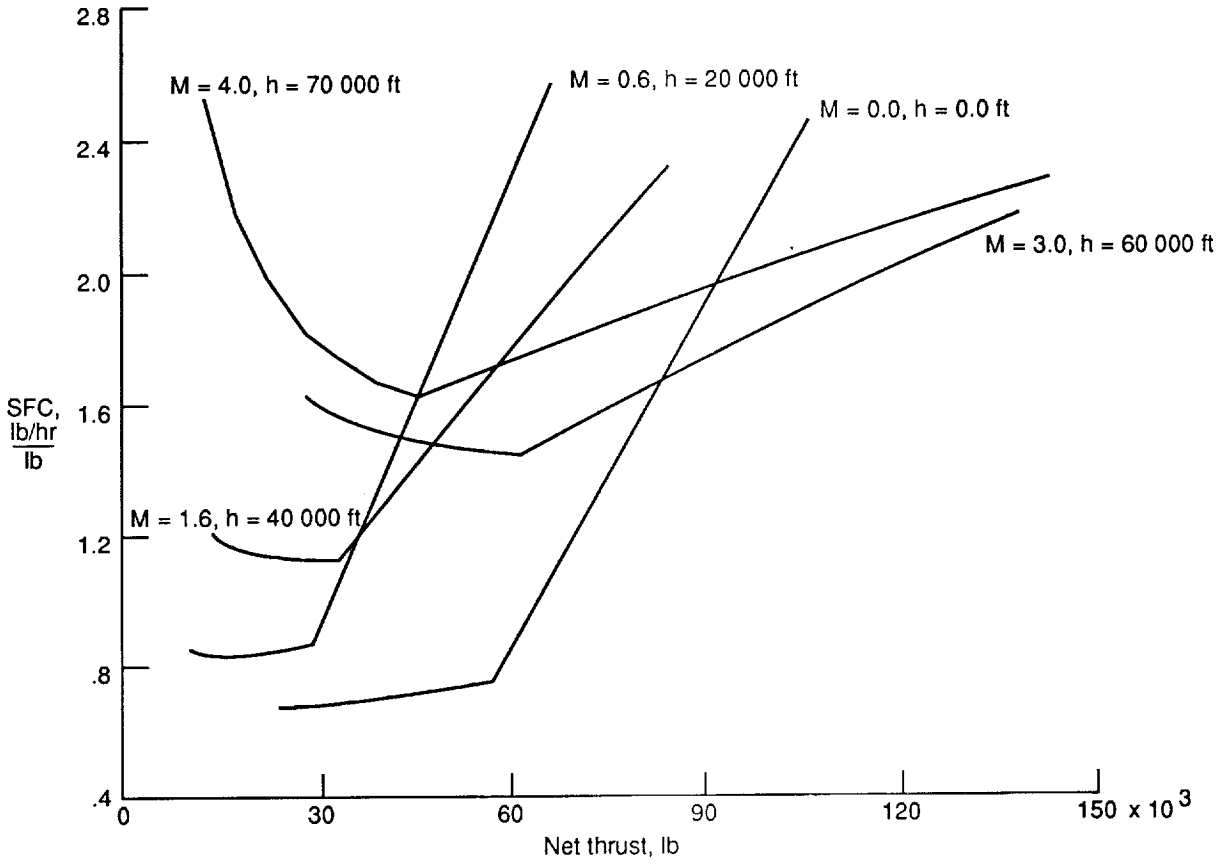

Figure 16. Installed engine SFC characteristics.

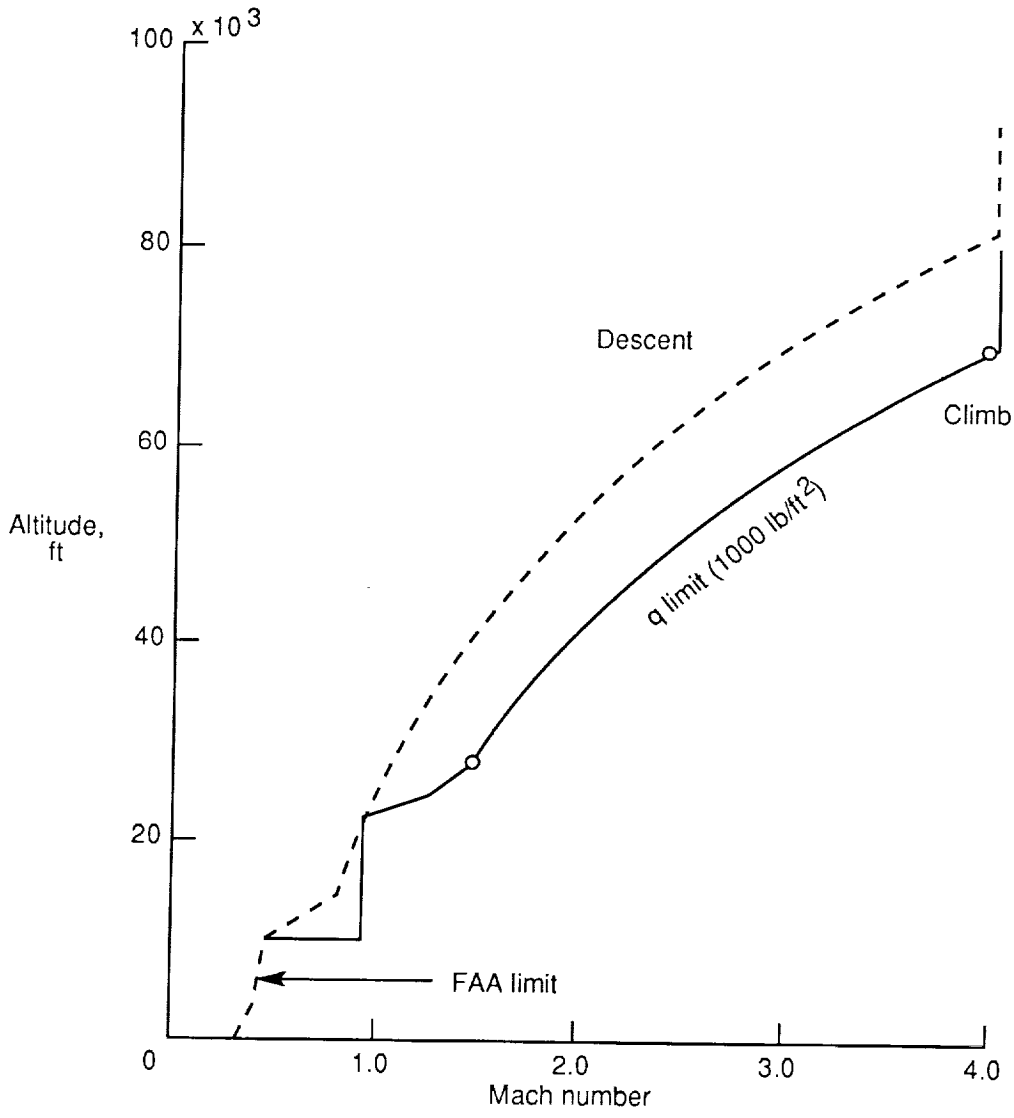

Figure 17. Climb and descent profiles.

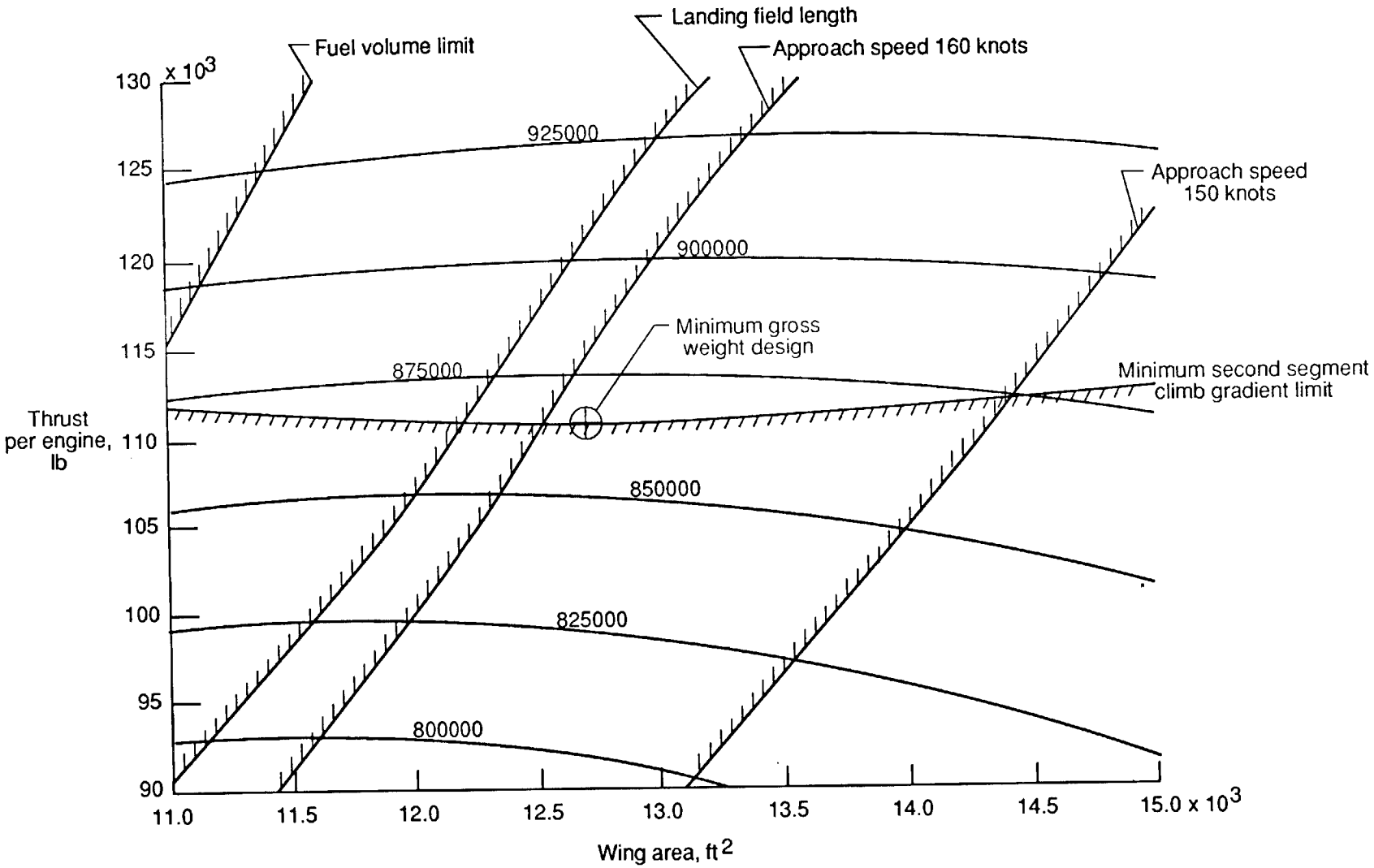

Figure 18. Thumbprint sizing plot.

NASA
National Aeronautics and Space Administration

Report Documentation Page

1. Report No.	2. Government Accession No.	3. Recipient's Catalog No.
NASA TM-4223		

4. Title and Subtitle
Concept Development of a Mach 4 High-Speed Civil Transport

5. Report Date
December 1990

6. Performing Organization Code

7. Author(s)
Christopher S. Domack, Samuel M. Dollyhigh, Fred L. Beissner, Jr., Karl A. Geiselhart, Marvin E. McGraw, Jr., Elwood W. Shields, and Edward E. Swanson

8. Performing Organization Report No.
L-16603

10. Work Unit No.
505-69-01-02

9. Performing Organization Name and Address
NASA Langley Research Center
Hampton, VA 23665-5225

11. Contract or Grant No.

13. Type of Report and Period Covered
Technical Memorandum

12. Sponsoring Agency Name and Address
National Aeronautics and Space Administration
Washington, DC 20546-0001

14. Sponsoring Agency Code

15. Supplementary Notes
Christopher S. Domack, Fred L. Beissner, Jr., Karl A. Geiselhart, Marvin E. McGraw, Jr., and Elwood W. Shields: Lockheed Engineering & Sciences Company, Hampton, Virginia.
Samuel M. Dollyhigh: Langley Research Center, Hampton, Virginia.
Edward E. Swanson: Planning Research Corporation, Hampton, Virginia.

16. Abstract

A study was conducted to configure and analyze a 250-passenger, Mach 4 high-speed civil transport with a design range of 6500 n. mi. The design mission assumed an all-supersonic cruise segment and no community noise or sonic boom constraints. The study airplane was developed in order to examine the technology requirements for such a vehicle and to provide an unconstrained baseline from which to assess changes in technology levels, sonic boom limits, or community noise constraints in future studies. The propulsion, structures, and materials technologies used in sizing the study aircraft were assumed to represent a technology availability date of 2015. The study airplane was a derivative of a previously developed Mach 3 concept and used advanced afterburning turbojet engines and passive airframe thermal protection. Details of the configuration development, aerodynamic design, propulsion system, mass properties, and mission performance are presented. The study airplane was estimated to weigh approximately 866 000 lb. Although an airplane of this size is a marginally acceptable candidate to fit into the world airport infrastructure, it was concluded that the inclusion of community noise or sonic boom constraints would quickly cause the aircraft to grow beyond acceptable limits with the technology levels assumed in the study.

17. Key Words (Suggested by Authors(s))	18. Distribution Statement
Supersonic cruise Aircraft design Transport aircraft	Unclassified—Unlimited Subject Category 05

19. Security Classif. (of this report)	20. Security Classif. (of this page)	21. No. of Pages	22. Price
Unclassified	Unclassified	28	A03

NASA-Langley, 1990
For sale by the National Technical Information Service, Springfield, Virginia 22161-2171